ANNUAL REPORT

SOLID STATE PHYSICS RESEARCH INSTITUTE

Virginia State University
Petersburg, VA 23803

Supported by NASA Grant NAG 1-416

Report Period: 1/1/85 - 12/31/85

Annual Report
Solid State Physics Research Institute
Virginia State University
Petersburg, VA 23803

Supported by NASA Grant NAG-1-416
Report Period: 1/1/85 - 12/31/85

The Solid State Physics Research Institute at Virginia State University was formally organized in January 1984 subsequent to the funding received through NASA grant NAG-1-416. The institute is a collection of three research programs. Two of these, muon spin rotation studies and studies of annealing problems in gallium arsenide, were funded previously by NASA through separate grants. The MuSR program was begun in 1972, while the GaAs studies were initiated in 1982. A third program, Hall effect studies in semiconductors, was initiated with the establishment of the institute. C. E. Stronach is director of the institute as well as P/I of the MuSR program. J. J. Stith and J. C. Davenport (VSU physics department chairman) are co-principal investigators of the GaAs program, while G. W. Henderson is P/I of the Hall effect program.

The purposes of this institute are threefold: (1) to perform state-of-the-art research in both basic and applied aspects of solid state physics which is both intrinsically interesting and which can be applied to problems of interest to NASA; (2) to develop a self-sustaining physics research program at VSU which will bring distinction to the university and its physics department; and (3) to provide training and experiences to students which will prepare them for careers in research.

The following sections describe the activities of each of the research programs during the period January 1 - December 31, 1985. Following this is a section describing activities which do not fall strictly within any of the three

programs, plus descriptions of student activities, equipment acquisitions, and future plans.

Muon Spin Rotation Studies

The muon spin rotation project efforts centered around experiments done at the Alternating Gradient Synchrotron of Brookhaven National Laboratory. Experiments and beam development done in 1983 and 1984 were followed by a number of experiments done in March/April and May/June 1985. These include studies of TiH_x and YH_2, TMMC, aluminum alloys, and heavy fermion superconductors. Appendix 1 is an abstract of a paper to be presented at the March 1986 American Physical Society meeting on the TiH_x results, along with a plot of the data. Appendix 2 is an abstract for an analogous paper on the aluminum alloy data.

Analysis of iron alloy data shows that the magnetic field sensed by the muon, B_μ, is greater in magnitude for Fe(Au) than for pure iron, but it is smaller in magnitude for Fe(Dy) and Fe(Ta). The effect is valence and hence electron density related and follows the "Doyama rule" which was first stated after analogous positron studies of alloys. That is, μ^+ (and e^+) are repelled by impurities to the right of iron in the periodic table, but are attracted by impurity atoms to the left of iron in the periodic table. The Fe(Ta) results are strongly dependent on sample preparation and a complete report on these materials awaits a study of Fe(Ta) alloys to be done at Brookhaven in May 1986 in which the shifts of B_μ upon annealing are analyzed in detail. An abstract of a paper presented on this topic at the March 1985 American Physical Society is

included as Appendix 3.

We are most pleased to report that the paper, "Uniaxial stress induced symmetry breaking for muon sites in Fe" was published in the July 1, 1985 issue of Physical Review B. This study was a major ongoing effort for about five years (1980-85) and was supported both by NAG-1-416 and the preceding grant NSG-1342. A reprint of this paper is included in this report as Appendix 4.

The principal investigator and two graduate students, Lucian Goode, Jr. and Nana Adu, visited the Saclay laboratory in France in June/July 1985 to study muon spin rotation in Ni and Ni(Pt) in conjunction with the French group led by Dr. Robert I. Grynszpan of the Center for the Study of Metallurgical Chemistry, Vitry-sur-Seine, France. The travel funds were provided by the USA/France Muon Spin Rotation Program, which is supported by the National Science Foundation. No NASA funds were used. The purpose of the experiment was to determine whether μ^+ in Ni(Pt) trap at sites near the Pt atoms for which B_μ is substantially different from that for pure Ni. An extensive study at 77K showed no such trapping.

The principal investigator served on the scientific advisory committee of the European Workshop on Subatomic Species in Solids, which was held in Vitry, France, September 2-6, 1985. He also gave a talk on "Quantum field theoretical aspects of muon spin rotation" at the meeting. Again, travel was supported by the NSF grant for the USA/France Muon Spin Rotation Program and no NASA funds were used. A digest of the talk is included here as Appendix 5.

Another round of μSR experiments is planned for May/June 1986. These are expected to include additional Fe(Ta) measurements, additional heavy fermion superconductor studies, fatigue studies in metals (in collaboration with our French colleagues), and studies of additional metal hydrides.

An experiment recently done at the KEK laboratory in Japan (and even more recently improved upon at the TRIUMF laboratory in British Columbia) bodes well for future μSR research, particularly with regard to its utilization in the study of surfaces. A low-energy μ^+ beam was projected onto tungsten foils. Three to five percent (20 to 25% at TRIUMF) of the incident μ^+ were subsequently desorbed with energies of a few electron volts. We plan to design a beam based on this phenomenon to provide extremely low energy μ^+ at the Alternating Gradient Synchrotron (Brookhaven) for studies of surfaces. Preliminary studies will commence during the May/June 1986 run.

Preparations for the 1986 run include development of the PDP 11/73 computer (programming, purchasing peripherals and software) and a cryogenics system for low-temperature studies. Electronic timing should be improved with the acquisition of a higher resolution time-to-amplitude converter and a constant-fraction discriminator.

The Virginia State University participants in these experiments were Carey E. Stronach, director of the institute, Lucian R. Goode, Jr., and Nana Adu, physics graduate students, and Michael R. Davis, an undergraduate physics major. The Brookhaven program is under the overall leadership of William J. Kossler, professor of physics at the College of William and Mary. Other participants included William F. Lankford of George Mason University, Harlan Schone of William and Mary, Gabriel Aeppli of Bell Laboratories, Alain Yaouanc of CNRS, Grenoble, France, Ola Hartmann and Roger Wäppling of the University of Uppsala, Sweden, Joseph Budnick of the University of Connecticut, and two graduate students from William and Mary.

During the past year three graduate students and one undergraduate participated in the radiation damage research project. A continuation of this level of student participation is anticipated for the coming year. John Stith, one of the principal investigators, attended two professional meetings during the year(The 1985 IEEE Annual Conference on Nuclear and Space Radiation Effects in Monterey, CA and The Eighteenth IEEE Photovoltaic Specialists Conference in Las Vegas, Nevada). A graduate student, Larry Brown, accompanied John Stith to the Nuclear and Space Radiation Effect Conference. A Late News Paper which was co-authored by John Stith of Virginia State University and John Wilson of NASA Langley Research Center was presented at the Photovoltaic Specialists Conference by John Stith. John Stith also spent approximately six weeks at the NASA Langley Research Center during the summer.

Graduate student participation is an essential component of the research grant. Presently, three graduate students are involved in research projects directly related to the radiation damage studies. These students will eventually use their findings or results to write theses which they will use as a part of their requirements for the Master of Science degree. One of these students is scheduled to graduate in May. His research project or thesis topic deals with an important aspect of radiation damage studies utilizing computer simulation studies. He has made a comparative study of the effect of using two different potential functions in the model used for the simulations. This study is an extremely significant aspect of radiation damage studies

utilizing computer simulation techniques since the interatomic potential is one of the most important parameters to be chosen in developing simulations models.

This aspect of the project demanded a great deal of time and input from the principal investigators who are associated with the radiation damage studies. Formal courses on radiation damage studies are not offered in the department, consequently the principal investigators must provide individualized instructions and supervision for these students participating on the project. Consequently, the project has served an important and informal mechanism for enhancing students' graduate training and experiences.

The radiation damage simulation research has been concentrating mostly on simulations of radiation damage produced in a gallium arsenide crystal when it is irradiated with protons and electrons. The simulations were performed with a modified version of the binary collision simulation code called MARLOWE. The modified version which has been described in an earlier report is referred to as MARS.[1] Approximately one hundred different computer runs were made during the year in order to build up a substantial data base and to test the substantial number of modifications that had to be made in the code to keep it compatible with the computer operating systems at NASA. These modifications were made necessary by the seemingly continuous upgrading of the computer system at NASA. In order to perform useful simulations with this code an acceptable and realistic

model was first developed for the gallium arsenide crystal. One of the most important aspects of the model is the selection of an interatomic potential function to be used for the interatomic interactions that are simulated. The Moliere and the Born-Mayer potential functions were considered because of the behavior of these two functions for relatively large nuclear separation(=>1 A^0) where the outer electron shells become important. These large nuclear separations are expected during collisions between a relatively low energy primary recoil atom and other atoms inside the crystal. The Moliere potential function is

$V(r)=((Z_1*Z_2*e^2)/r)*f(r)$

$f(r)=(0.35*\exp(-0.30*r/a)+0.55*\exp(-1.2*r/a)+0.10*\exp(-6.0*r/a))$

where 'a' is the screening radius and 'r' is the interatomic separation. The Born-Mayer potential function is

$V(r) = A\exp(-r/a_B)$ where 'r' is the interatomic separation, 'a_B' is the screening radius and the average value of 'A' for gallium arsenide is 9,413 eV. Plots of the Moliere and Born-Mayer potential functions for a range of interatomic separations are shown in figure 1. The Born-Mayer potential function was finally selected as the function to be used in the model because of the way in which it approaches zero at relatively large interatomic separation and the fact that it was derived from experimental results.

The simulation code has been used to generate results for radiation produced damage in gallium arsenide by keeping track of the action of a simulated primary recoil atom as it moves among the lattice sites of the crystal. The primary recoil atoms are

given a range of energies corresponding to some of the possible energy transfers from 1-MeV electrons to atoms of gallium or arsenic. The maximum transfer from the 1-MeV electron is approximately 65 eV. The 1-MeV electron was chosen because of its importance in equivalent electron fluence studies[2].However, further studies performed during the year on the concept of equivalent electron fluence yielded results that indicated that 1-MeV electrons should be replaced by 10-MeV electrons in order to make the equivalent electron fluence concept more valid. The studies are described in greater detail in reference 4. A copy of reference 4 is included in the appendix of this report.

The results from the simulations include the following: a. number of displaced atoms; b. number of improper replacements; c. number of improper replacements; d. number of proper replacements; e. inelastic energy loss; f. range of the primary recoil atom; g. number of interstitials atoms; h. number vacancies; and i. number of Frenkel pairs.

A theorectical understanding of displacement effects in semiconductors requires a detailed analysis of the dependence of the quantities listed above on the energies of the primary recoil atoms. This analysis is done by plotting graphs and studying the relationship between the various results from the simulated radiation and the energy of the primary recoil atoms. These graphs represent some interesting and important results. A graph of the total number of displacements versus energy in figure 2 indicates an approximately linear relationship between the total number of displacements and the energy of the primary recoil atom

for the range of energies used in the simulations. Curve 2 in this figure was plotted using results obtained from a computational model developed earlier by Wilson, Stith, and Stock[3]. Curve 3, included in this figure, represents a plot of the number of Frenkel pairs versus energy. Figure 3 is a plot of the inelastic energy losses of the primary recoil atoms versus the initial energies of the primary recoil atoms. Figure 4 is a plot of the ratios between the inelastic energy losses and the initial energies of the primary recoil atoms versus the initial energies of the primary recoil atoms. From the graph in figure 4 it appears that the percentage of the primary recoil atoms' energies that is lost during inelastic collisions approaches a maximum of approximately 20 percent. Figure 5 is a plot of the total number of defects versus energy. The total number of defects is the sum of the number of improper replacements, the number of interstitial atoms, and the number of vacancies.

Further studies will be made on the above results during the coming year. A study of the effect of temperature on the production of defects will be included.

References

1. Annual Report of the Solid State Physics Research Institute, Virginia State University; Petersburg,Virginia. Report Period: 1/1/84-12/31/84
2. Wilson, John; Stith, John; and Walker, Gilbert: Sixteenth IEEE Photovoltaic Specialists Conference-1982, 82CH1821-8, 1982, pp. 1439-1440.
3. Wilson, John; Stith, John; and Stock, Larry: NASA Technical Paper 2242, December 1983.
4. Stith, John and Wilson, John; Microscopic Defect Structures and Equivalent Electron Fluence Concepts. Presented at the 1985 IEEE Specialists Conference, October 1985.

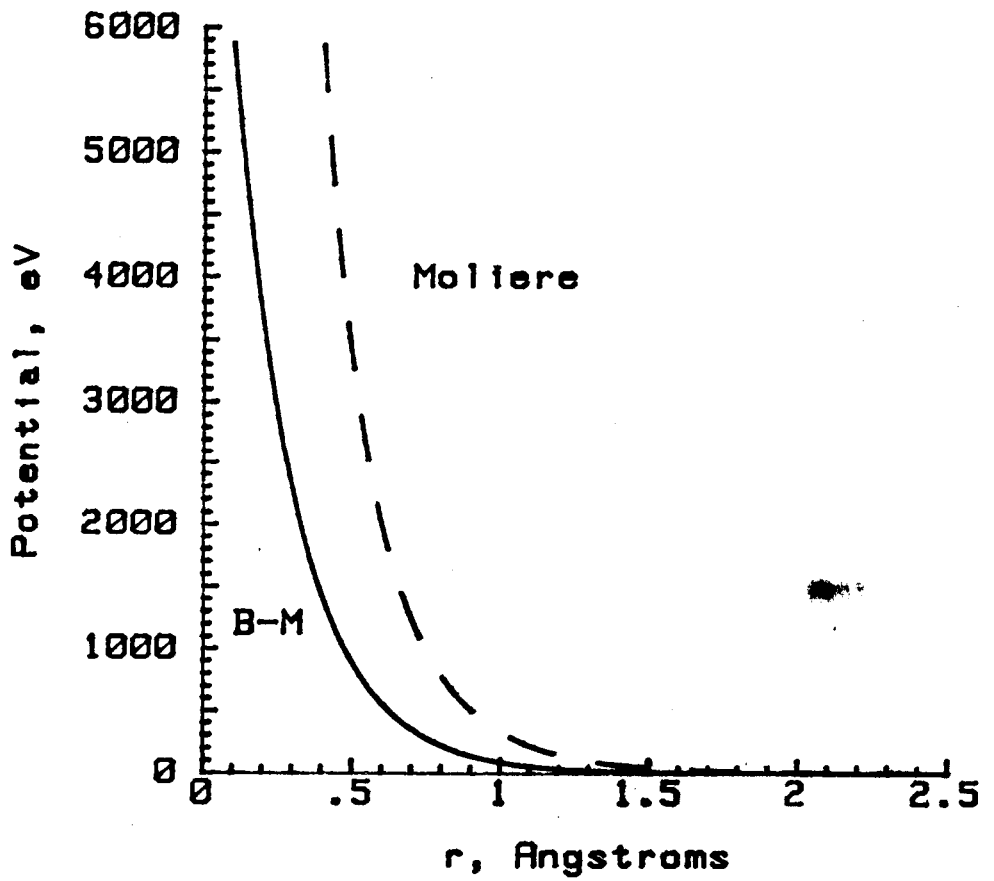
6000
5000
4000
3000
2000
1000
0
Potential, eV
Moliere
B-M
0
.5
1
1.5
2
2.5
r, Angstroms

figure 1

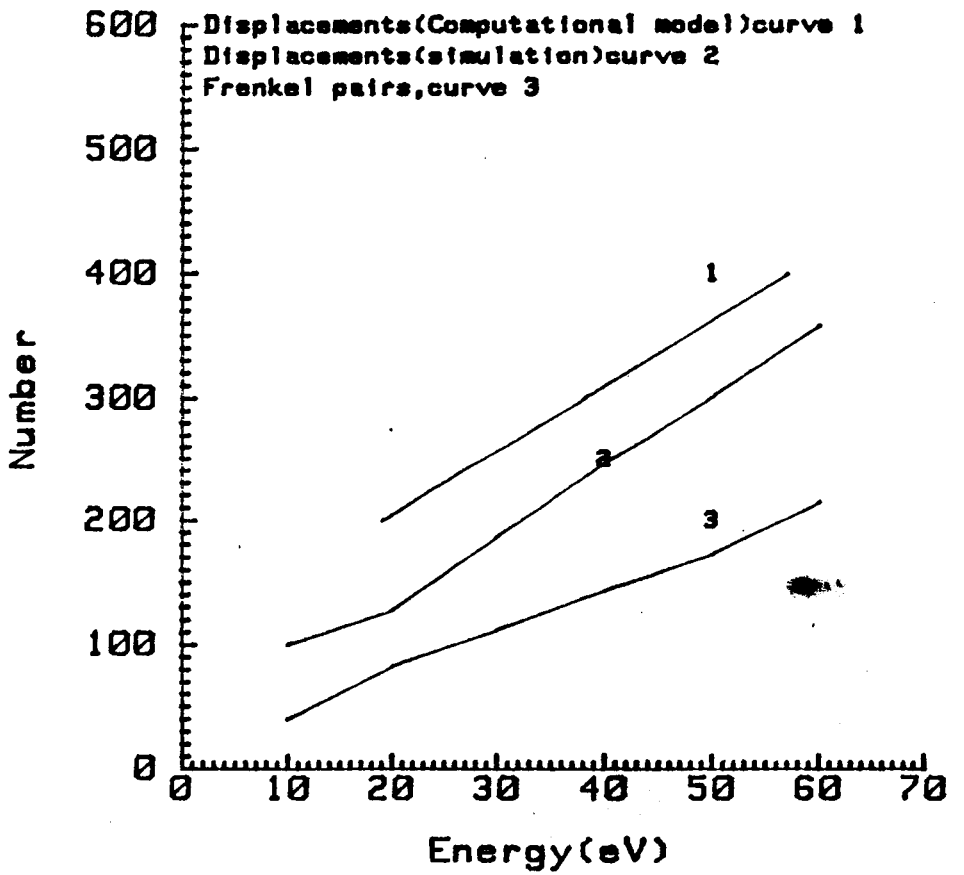
Displacements(Computational model)curve 1
Displacements(simulation)curve 2
Frenkel pairs,curve 3
600
500
400
300
200
100
0
Number
1
2
3
0
10
20
30
40
50
60
70
Energy(eV)

Figure 2

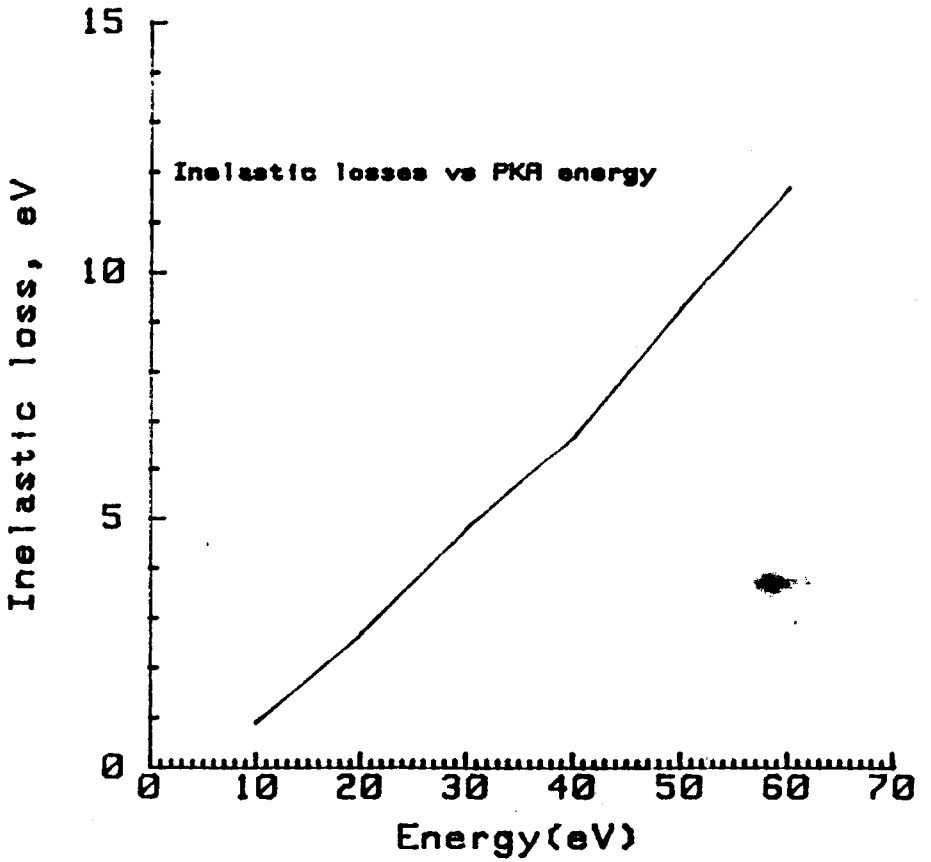
Inelastic losses vs PKA energy
Inelastic loss, eV
15
10
5
0
0
10
20
30
40
50
60
70
Energy(eV)

Figure 3

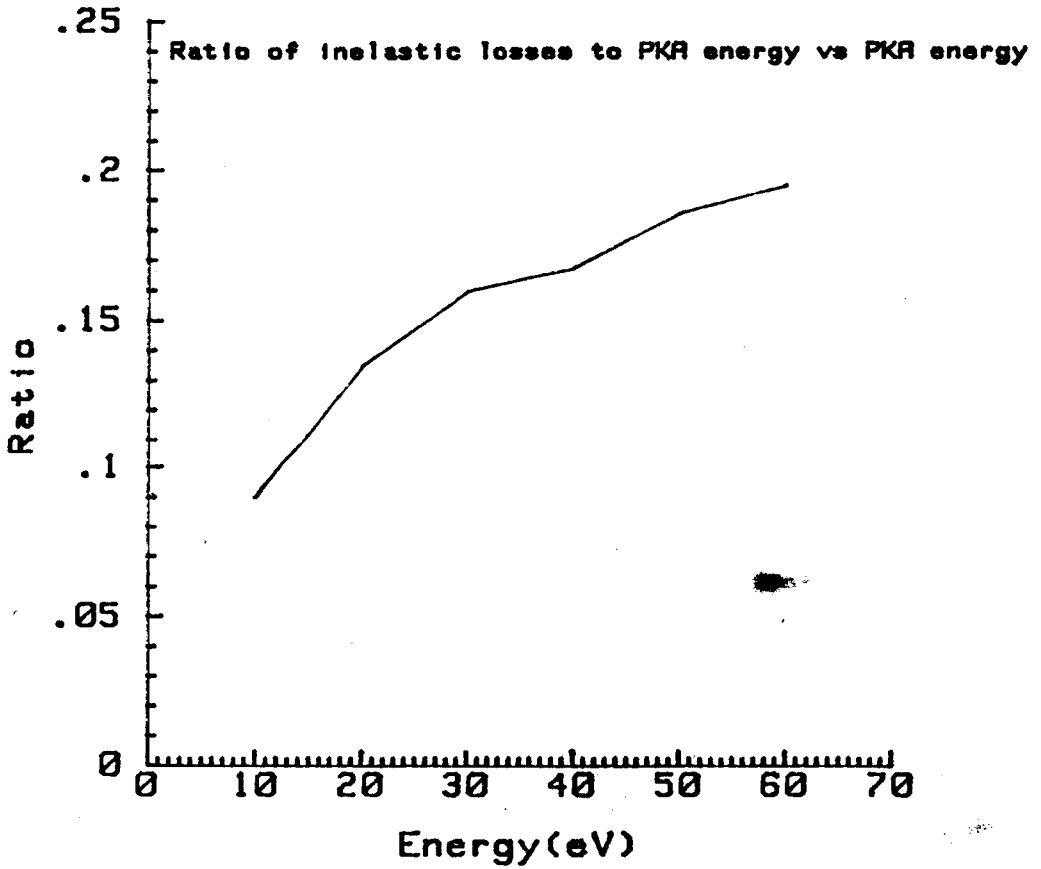
Ratio of inelastic losses to PKA energy vs PKA energy
.25
.2
.15
.1
.05
0
Ratio
0
10
20
30
40
50
60
70
Energy(eV)

Figure 4

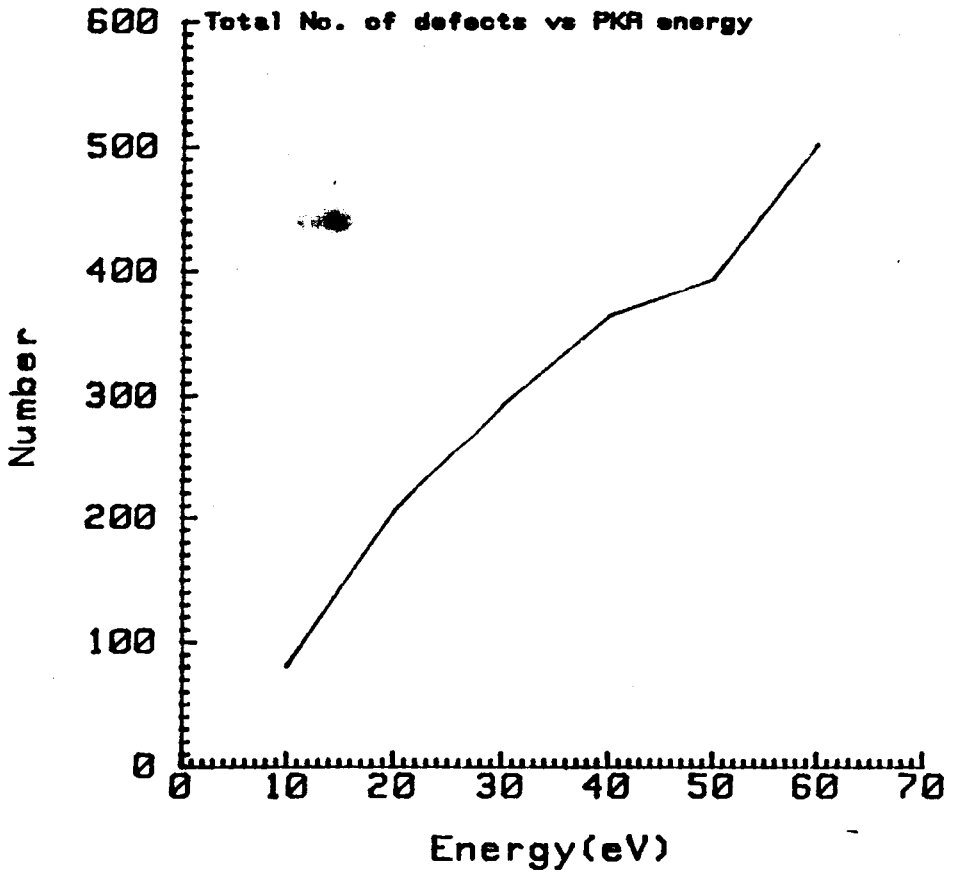
Total No. of defects vs PKA energy
600
500
400
300
200
100
0
Number
0
10
20
30
40
50
60
70
Energy(eV)

Figure 5

THE HALL EFFECT ANNUAL REPORT

During the year the Hall effect research program moved through several milestones. The equipment was acquired which will allow conventional Hall effect measurement to be made at Virginia State University. The program involved two undergraduates and one graduate students in the system development. A working relationship was developed with the Naval Research Laboratory was also commenced. This contact will allow the performance of Quantum Hall effect.

We also consulted Dr. Robert Coleman at the University of Virginia. He is during Hall Effect experiments. The principal investigator also attended a short course in Radiation Damage through the auspices of the IEEE a Monterey, California.

The measurement system at Virginia State University consists of a Walker Scientific Power supply (from 0 to 50 amp), an alpha Magnet, a digital Gaussmeter, a HP 9816 computer with peripherals, a 3497A data acquisition will be used to acquire and analyze the data. A cryostat has also been acquired.

Roscoe Ledbetter, an undergraduate student has developed a computer program for data acquisition. A program to process and analyze the data is nearing completion. The decision has been made to operate two systems of sample geometries. One

employs the standard Hall sample configuration. The other will utilize the Van der Pauw technique.

The experimental procedure as we have perceived it consists of the measurement of the Hall coefficient, resistivity, and Hall mobility as a function of temperature of a sample of Gallium Arsenide before and after irradiation with low and high energy protons. In order to compare the results with the known damages that are produced by proto irradiation , one need to know the relationship among the quantities that radiation damage and the Hall effect measurements have in common.

It is known that the effect of radiation damage is associated with the carrier concentration and the Hall mobilities . The manifestation of the radiation defects are "intrinsic defects". In order to establish and test the theory , a theoretical model is being developed using Lindhard's theory of atomic collisions.

The second most important step is to link the quantum Hall effect and the changes produced by proton collisions. Work has begun on the the development of a theory and subsequently experiments will be designed and performed.

APPENDIX I
RESISTIVITY AND HALL COEFFICENT MEASUREMENTS
VAN DER PAUW METHOD

The measurement theory developed by Van der Pauw involves the use of arbitrary geometric configurations . Incumbent adjustments are made for the chosen geometry. For our system consider a lamella

In order to make resistivity measurements a current I is passed through two adjacent contacts e.g. (2 and 3), the voltage V is then measured across the other contacts. The equation R = V/I is used. Next a current I' is passed through the next pair of contacts (3,4) and the voltage V' is measured across the other contacts. The equation R' = V'/I' is used. The resistivity ' ' of sample of thickness 't' is related to R and R' through the relation Exp(- tR/) + Exp(- tR'/) = 1. The resistivity can thus be obtained.

In order to determine the value of the Hall coefficient, a current I is passed through two non adjacent contacts and the voltage V is measured across the other two. The relation R = R/I is used. The magnetic field is now energized and the measurements of V' and I' are then made on the same contacts. The Hall coefficient R_H can now be determined from u = R_H/ .

The measurement process consists passing a current through both directions and averaging the results. The magnetic field is reversed and measurements taking in both direction and averaged.

The following relations are typical for the experimental determination of the resistivity and Hall mobility. All measurement are made as a function of temperature.

$$= t/\ln 2(V_{23}/2I_{14} + V_{24}/2I_{31})\, f$$

$$u_H = (V^H_{32})2\ln 2/\ B(V_{21}/I_{34} + V_{13}/I_{42})f$$

```
10    ! CURVE FITTING PROGRAM FOR HALL EFFECT DATA HENDERSON JORDAN FEB 7,1986
11    ! IDENTIFIERS
13    !     C1      COEF          SOLUTION VECTOR
14    !     C3      CORREL        CORRELATION COEFFICIENTS
15    !     E2      SIGMA         VECTOR OF ERRORS
16    !     E5      SEE           STD ERROR OF ESTIMATE
17    !     L3      NLIN          NUMBER OF PLOT LINES
18    !     M1      MAX           MAXIMUM LENGTH
19    !     N1      NROW          NUMBER OF ROWS
20    !     N2      NCOL          NUMBER OF COLUMNS
21    !     R3      RESID         VECTOR OF RESIDUALS
22    !     S7      SUMY          SUM OF Y
23    !     S8      SUMY2         SUM OF Y SQUARED
24    !     T6      SRS           SUM OF RESIDUALS SQUARED
25    !     Y3      YCAL          CALCULATED Y
26    ! END OF IDENTIFIERS
40    A$="DDD  DD.D  "
50    C$="DDD   DD.d"
60    M1=35
70    DIM Z(4),A(4,4),C1(14),Y(35),U(35,4)
80    DIM W(4,1),B(4,4),I2(24,23),X(35),Y1(35)
90    DIM Y2(35),R3(35),E2(4)
100   GRAPHICS OFF
110   PRINT
120   PRINT " UP TO THIRD DEGREE POLYNOMIAL  LEAST SQUARES FIT BY GAUSS JORDAN E
LIMINATION"
130   PRINT
140   GOSUB 500      ! GET THE DATA
150   ! SORT THE DATA
160   GOSUB 800       !  SQUARE UP THE MATRIX
170   GOSUB 4000      !  SET UP THE MATRIX
180   GOSUB 5000      !  GAUSS-JORDAN SOLUTION
190   GOSUB 1000      !  PRINT THE RESULTS
200   GOSUB 7000      !  PLOT DATA
210   GOTO 100
500   !  GET THE DATA
510   INPUT "NUMBER OF DATA POINTS",N1
520   INPUT "POLYNOMIAL ORDER",N2
530   IF N2>3 THEN 520
540   IF N2<1 THEN 9999
550   N2=N2+1
560 L3=(N1-1)*2+1
570   IF N4=1 THEN 620
580   FOR I=1 TO N1
600   READ X(I),Y1(I)
610   NEXT I
620   RETURN
630   ! Y DATA
640   DATA 1,2.07,2,8.6,3,14.42,4,15.8,5,18.92,6,17.96
650   DATA 7,12.98,8,6.45,9,.27
660   RETURN   ! FROM INPUT ROUTINE
800   ! SET UP THE MATRIX DATA
810   FOR I=1 TO N1
820   U(I,1)=1
830   FOR J=2 TO N2
840   U(I,J)=U(I,J-1)*X(I)
850   NEXT J
860   Y(I)=Y1(I)
870   NEXT I
```

```
0990   RETURN    ! FROM SETTING UP DATA MATRIX
1000!  CALCULATE RESIDUALS AND PRINT RESULTS
1001 PRINTER IS 701
1010  S7=0
1020  S8=0
1030  T6=0
1040  FOR I=1 TO N1
1050  Y3=0
1060  FOR J=1 TO N2
1070  Y3=Y3+C1(J)*U(I,J)
1080  NEXT J
1090  R3(I)=Y3-Y(I)
1100  Y2(I)=Y3
1110  T6=T6+R3(I)^2
1120  S7=S7+Y(I)
1130  S8=S8+Y(I)^2
1140  NEXT I
1150  C3=SQR(1-T6/(S8-S7^2/N1))
1160  IF N1=Ns THEN E5=SQR(T6)
1170  IF N1<>N2 THEN E5=SQR(T6/(N1-N2))
1180  FOR J=1 TO N2
1190  E2(J)=E5*SQR(ABS(B(J,J)))
1200  NEXT J
1210  PRINT "          X          Y         YCAL          RESID"
1220  FOR I=1 TO N1
1230  PRINT USING "5X,DD,6X, DDD.DD,6X,DDD.DD,6X,DDD.DD,6X,DDD.DD";I,X(I),Y(I),Y
2(I),R3(I)
1240  NEXT I
1250  PRINT
1260  PRINT "COEFFICIENT      ERRORS"
1270  PRINT USING "5X,DDD.DD,3X,DDD.DD";C1(1),E2(1)
1290  FOR I=2 TO N2
1300  PRINT USING "5X,DDD.DD,3X,DDD.DD";C1(I),E2(I)
1310  NEXT I
1320  PRINT
1330  PRINT USING "10X,27A,1X,DDD.DD";"CORRELATION COEFFICIENT IS",C3
1331  PRINT
1332  PRINT
1333  PRINT "EQUATION  OF CURVE"
1334  PRINT USING "10X,DDD.DD,1X,1A,1X,DDD.DD,1A,1X,1A,1X,DDD.DD,3A,1X,1A,DDD.DD
,5A";C1(1),"+",C1(2),"X","+",C1(3),"X*X","+",C1(4),"X*X*X"
1336  WAIT 10
1337  PRINTER IS 1
1340  RETURN ! FROM PRINTOUT
4000  ! U AND Y CONVERTED TO A AND Z
4011  ! IDENTIFIERS
4013  !    N1      NROW      NUMBER OF ROWS
4014  !    N2      NCOL      NUMBER OF COLUMNS
4015  !    END OF IDENTIFIERS
4020       FOR K=1 TO N2
4030       FOR L=1 TO K
4040       A(K,L)=0
4050       FOR I=1 TO N1
4060       A(K,L)=A(K,L)+U(I,L)*U(I,K)
4070       IF K<>L THEN A(L,K)=A(K,L)
4080       NEXT I
4090       NEXT L
4100       Z(K)=0
4110       FOR I=1 TO N1
4120       Z(K)=Z(K)+Y(I)*U(I,K)
4130       NEXT I
4140       NEXT K
5000       !  JORDAN MATRIX INVERSION AND SOLUTION
5010       !  FEB  7, 1986
5011       !    IDENTIFIERS
5012       !    A       A       COEFFICIENT MATRIX
```

```
5014        !     B1      BIG      BIGGEST VALUE
5015        !     C1      COEF     SOLUTION VECTOR
5016        !     D3      DETERM   DETERMINANT
5017        !     E1      ERMES    ERROR FLAG
5018        !     H1      HOLD     WORK VARIABLE
5019        !     I2      INDEX    WORK MATRIX
5020        !     I3      IROW     ROW  INDEX
5021        !     I4      ICOL     COLUMN INDEX
5022        !     I5      INVRS    PRINT- INVERSE FLAG
5023        !     N2      NCOL     NUMBER OF COLUMNS
5024        !     N3      NVEC     NUMBER OF CONSTANT VECTORS
5025        !     P1      PIVOT    PIVOT INDEX
5026        !     W       W        SOLUTION MATRIX
5027        !     Z       Z        CONSTANT VECTOR
5029        !     END OF IDENTIFIERS
5080        !
5090        E1=0 ! BECOMES 1 FOR SINGULAR MATRIX
5100        I5=1 ! PRINT INVERSE MATRIX IF ZERO
5110        N3=1 ! NUJMBER OF CONSTANT VECTORS
5120        FOR I=1 TO N2
5130        FOR J=1 TO N2
5140        B(I,J)=A(I,J)
5150        NEXT J
5160        W(I,1)=Z(I)
5170        I2(I,3)=0
5180        NEXT I
5190        D3=1
5200        FOR I=1 TO N2
5210        !
5220        !  SEARCH FOR LARGEST (PIVOT) ELEMENT
5230        !
5240        B1=0
5250        FOR J=1 TO N2
5260        IF I2(J,3)=1 THEN 5350
5270        FOR K=1 TO N2
5280        IF I2(K,3)>1 THEN 6120
5290        IF I2(K,3)=1 THEN 5340
5300        IF B1>=ABS(B(J,K)) THEN 5340
5310        I3=J
5320        I4=K
5330        B1=ABS(B(J,K))
5340        NEXT K
5350        NEXT J
5360        I2(I4,3)=I2(I4,3)+1
5370        I2(I,1)=I3
5380        I2(I,2)=I4
5390        !  INTERCHANGE ROWS TO PUT PIVOT ON DIAGONAL
5400        IF I3=I4 THEN 5540
5410        D3=-D3
5420        FOR L=1 TO N2
5430        H1=B(I3,L)
5440        B(I3,L)=B(I4,L)
5450        B(I4,L)=H1
5460        NEXT L
5470        IF N3<1 THEN 5540
5480        FOR L=1 TO N3
5490        H1=W(I3,L)
5500        W(I3,L)=W(I4,L)
5510        W(I4,L)=H1
5520        NEXT L
5530        ! DIVIDE PIVOT ROW BY ELEMENT
5540        P1=B(I4,I4)
5550        D3=D3*P1
5560        B(I4,I4)=1
5570        FOR L=1 TO N2
```

```
5590        NEXT L
5600        IF N3<1 THEN 5660
5610        FOR L=1 TO N3
5620        W(I4,L)=W(I4,L)/P1
5630        NEXT L
5640        !
5650        ! REDUCE NONPIVOT ROWS
5660        FOR L1=1 TO N2
5670        IF L1=I4 THEN 5770
5680        T=B(L1,I4)
5690        B(L1,I4)=0
5700        FOR L=1 TO N2
5710        B(L1,L)=B(L1,L)-B(I4,L)*T
5720        NEXT L
5730        IF N3<1 THEN 5770
5740        FOR L=1 TO N3
5750        W(L1,L)=W(L1,L)-W(I4,L)*T
5760        NEXT L
5770        NEXT L1
5780        NEXT I
5790        !
5800        !  INTERCHANGE COLUMNS
5810        !
5820        FOR I=1 TO N2
5830        L=N2-I+1
5840        IF I2(L,1)=I2(L,2) THEN 5920
5850        I3=I2(L,1)
5860        I4=I2(L,2)
5870        FOR K=1 TO N2
5880        H1=B(K,I3)
5890        B(K,I3)=B(K,I4)
5900        B(K,I4)=H1
5910        NEXT K
5920        NEXT I
5930        FOR K=1 TO N2
5940        IF I2(K,3)<>1 THEN 6120
5950        NEXT K
5960        E1=0
5970        FOR I=1 TO N2
5980        C1(I)=W(I,1)
5990        NEXT I
6000        IF I5=1 THEN 6140
6010        PRINT
6020        PRINT "  MATRIX INVERSE"
6030        FOR I=1 TO N2
6040        FOR J=1 TO N2
6050        PRINT USING "10X,DDD.D";B(I,J)
6060        NEXT J
6070        PRINT
6080        NEXT I
6090        PRINT
6100        PRINT "DETERMINANT =",D3
6110        RETURN  ! IF INVERSE IS PRINTED
6120        E1=1
6130        PRINT "ERROR-MATRIX SINGULAR"
6140        RETURN ! FROM GAUSS-JORDAN SUBROUTINE
7000  PRINT "DO YOU WANT A GRAPH OF THE FUNCTION  (Y/N)"
7001  INPUT K$
7002  IF K$="Y" THEN 7009
7003  IF K$="N" THEN 9999
7009  ! PLOT OF Y AND Y2 AS A FUNCTION OF X, FEB. 5,1985
7010  C$=CHR$(255)&"K"
7020  DUMP DEVICE IS 701,EXPANDED
7030  OUTPUT 2 USING "#,K";C$       ! Clear leftover display
7040  PRINT
```

```
7050  PRINT
7060  OUTPUT 2 USING "#,K";C$        ! Clear screen for graph
7070  PRINT "WHAT X AND Y LABELS DO YOU WANT ON GRAPH"
7080  INPUT T1$,T$
7081  INPUT "MAXIMUM X,Y",N4,N5
7090  GINIT                          ! Initialize various graphics parametersGRAP
7100  PLOTTER IS CRT,"INTERNAL"      ! Use the internal screenGRAPHICS OFF
7110  GRAPHICS ON                    ! Turn on the graphics screenGRAPHICS OFF
7120  X_gdu_max=100*MAX(1,RATIO)     ! Determine how many GDUs wide the screen is
7130  Y_gdu_max=100*MAX(1,1/RATIO)   ! Determine how many GDUs high the screen is
7140  LORG 6                         ! Reference point: center of top of label
7150  DEG                            ! Angular mode is degrees (used in LDIR)
7160  LDIR 90                        ! Specify vertical labels
7170  CSIZE 4.5                      ! Specify smaller characters
7180  MOVE 0,Y_gdu_max/2             ! Move to center of left edge of screen
7190  LABEL T$        ! Write Y-axis label
7200  LORG 4                         ! Reference point: center of bottom of label
7210  LDIR 0                         ! Horizontal labels again
7220  MOVE X_gdu_max/2,.07*Y_gdu_max! X: center of screen; Y: above key labels
7230  LABEL T1$          ! Write X-axis labelGRAPHICS OFF
7240  VIEWPORT .1*X_gdu_max,.98*X_gdu_max,.15*Y_gdu_max,.9*Y_gdu_max
                                     ! Define subset of screen area
7250  FRAME                          ! Draw a box around defined subset
7260  WINDOW 0,N4,0,N5
7270  AXES 1,1,0,0,10,10,5    ! Draw axes with appropriate ticks
7280  CLIP OFF                       ! So labels can be outside VIEWPORT limits'
7290  CSIZE 1.6,1.6                  ! Smaller chars for axis labelling
7300  LORG 6                         ! Ref. pt: Top center      !\
7310  FOR I=0 TO N4 STEP N4/10       ! Every 10 units           ! \
7320    MOVE I,-.1                   ! A smidgeon below X-axis  !  > Label X-axis
7330    LABEL USING "#,DD.D";I       ! Compact; no CR/LF        ! /
7340  NEXT I                         ! et sequens               !/
7350  LORG 8                         ! Ref. pt: Right center     !\
7360  FOR I=0 TO N5 STEP N5/10       ! Every quarter            ! \
7370    MOVE -.05,I                   ! Smidgeon left of Y-axis  !  > Label Y-axi
s
7380    LABEL USING "#,DD.D";I   ! DD.D; no CR/LF           ! /
7390  NEXT I                         ! et sequens                !/
7400  PENUP
7410  I=0
7420  FOR I=1 TO N1
7430     PLOT X(I),Y(I)
7440  NEXT I
7450  MOVE 0,0
7460  FOR K=1 TO N1
7470  PLOT X(K),Y2(K)
7480       NEXT K
7490  PRINT "IF YOU WANT A HARD COPY OF GRAPH PRESS DUMP GRAPHICS"
7491  PRINT "IF NOT PRESS CONTINUE"
7492  PAUSE
7493  GRAPHICS OFF
7500  PRINT "DO YOU WANT TO PLOT ANOTHER SET OF DATA Y/N"
7510  INPUT Z$
7520  LABEL TIME$(TIMEDATE),DATE$(TIMEDATE)
7530  IF Z$="Y" THEN 100
7540  IF Z$="N" THEN 9999
7550  RETURN
7560  GRAPHICS OFF
7570   OUTPUT 2 USING "#,K";C$
9999  END
```

REFERENCE

B. V. Shemaev
Changes in the Electrophysical characteristics of n-type Silicon as a Result of Irradiation with 6.3 Mev Protons
Sov. Phys. Semicond. 18(2) February 1984

B. V. Shemaev
Positions of Acceptor levels of Divacancy in the band gap of n-type Silicon irradiated with 6.3 Mev Protons
Soviet Phy. Semicond. 18(2) February 1984

J. Lindhard, M. Scharf and H. E. Schiott
Range Concepts and Heavy Ions
Mat. Fys. Medd. Dan. Vid. Selsk. 33 no. 14 (1963)

Student Participation

During the Spring 1985 semester six graduate students were participating in the program, Lucian R. Goode, Jr., Akpan E. Akpan, Nana Adu, William Bolden, Larry Brown and Karamali Shojaei. Goode, Adu and Shojaei are working on MuSR projects; Akpan, Bolden and Brown are working on computer modeling of radiation damage in solids. In September 1985 another graduate student, Li-Tai Song, joined the institute and is working on Hall effect studies.

During the Spring 1985 semester four undergraduate students participated, Michael Davis, Roscoe Ledbetter, Cornelia Belsches and Raymond Noel. Fall 1985 undergraduates were Davis, Ledbetter, Belsches and Tony Barnes.

Other Activities

The director of the institute participated in an experiment on inelastic scattering of polarized protons from ^{12}C at the Los Alamos Meson Physics Facility in New Mexico during July/August and November/December 1985. Karamali Shojaei, a VSU graduate student, participated in the July/August run. Other collaborators included Bernard J. Lieb of George Mason University, Herbert O. Funsten, Charles F. Perdrisat and J. Michael Finn of the College of William and Mary, Hans S. Plendl of Florida State University, Joseph Comfort of Arizona State University, and one graduate student each from William and Mary, Florida State and Arizona State.

An abstract of a paper to be presented at the April 1986 APS meeting is included as Appendix 6. We are seeking other sources of funding for our participation in these experiments and hope for success in the near future.

Two papers based on work done at the Tri-University Meson Facility (Vancouver, BC) in 1979-80 and supported in part by NASA grant NSG 1646 were completed in

1985 with extremely minor support from NAG-1-416. Both were accepted for publication by Physical Review C. "Energy dependence of the $^{7}Li(p,d)^{6}Li$ reaction" appeared in the September 1985 issue and a reprint is included here as Appendix 7. "$^{4}He(\vec{p},d)^{3}He$ reaction at 200 and 400 MeV" is scheduled to appear in the February 1986 issue and a preprint is included here as Appendix 8.

The director participated in the revision of a paper based on pion-nucleus reaction experiments conducted at LAMPF in 1980 and supported in part by NASA grant NSG-1646. This revised version has been submitted to Physical Review C and a preprint is included here as Appendix 9.

The director of the institute has served as the Virginia State University representative on the board of trustees of the Southeastern Universities Research Association since October 1983. During 1985 he served on the SURA industrial affiliates committee and in early January 1986 was appointed to the science and technology committee of SURA. This committee will provide SURA oversight for the Continuous Electron Beam Accelerator Facility, which is a 4-GeV continuous wave electron accelerator to be constructed in Newport News, Virginia.

In May 1985 the director completed a one-year term as chairman of the astronomy, mathematics and physics section of the Virginia Academy of Science. He was also appointed to the local organizing committee for the International Symposium on the Physics and Chemistry of Small Clusters, which will take place in October 1986 in Richmond, Virginia.

James C. Davenport served as director of the summer student program at Fermilab (Batavia, Illinois) during the summer of 1985. He also served on the Committee on Minorities in Physics of the American Physical Society this past year.

George W. Henderson, John J. Stith and Larry D. Brown (graduate student) received course credit in the summer of 1985 for an IEEE-NSRE tutorial short course on radiation effects through the New Jersey Institute of Technology.

Equipment and Supplies

The following items were purchased during the reporting period:

- 1 Janis supertran helium transfer tube
- 4 EMI 9907B photomultiplier tubes
- 3 Ortec 265 tube bases
- 3 Ortec 218 phototube shields
- 1 EG&G/Ortec 567 Time-to-amplitude converter
- 1 PDP 11/73 computer (1-megabyte memory, 31-megabyte hard disk drive, dual floppy disk drives, terminal and printer
- 1 Interface Standards IS-11/CC CAMAC crate controller
- 2 Keithley 175 multimeters
- 1 Keithley 197 multimeter
- 3 Hewlett-Packard HP-15C calculators
- 100 reprints of our paper on MuSR in strained single crystals of iron
- 1 1-megabyte memory board for HP 9816S computer
- 1 Hewlett-Packard terminal emulator
- 1 Hewlett-Packard 9816S computer with accessories
- 1 Hewlett-Packard HP 3497A data acquisition control unit
- 1 MICRO/RSX operating system for PDP-11/73 computer
- 3 PVC inserts and magnetic shields for phototubes

In addition, the internal account at Brookhaven National Laboratory was continued in force. This enables the institute to purchase equipment, supplies and materials from BNL directly while experiments are in progress.

Three peripherals for the PDP 11/73 computer were ordered (plotter, modem, line filter) and received in early 1986. Several others (IEEE bus, INVERTER, and Advanced Programmers Kit) are still on order. A quadruple constant fraction discriminator and a scientific word processing program are also on order.

Summary

The second year of support from NASA for the Solid State Physics Research Institute was a year of growth and consolidation. The MuSR program saw a major publication, substantial progress on several other projects and near completion of the new data acquisition and analysis system (which should be complete in time for experiments in the spring of 1986. The radiation damage studies have gone into production mode, and the Hall effect apparatus is essentially complete. The number of student participants increased substantially over the 1984 level.

The higher level of student interest has enabled the principal investigators to set higher standards for student eligibility for research stipends, and the quality of student involvement showed marked improvement as we began the spring 1986 semester.

We look forward to another active and successful year in 1986, and we appreciate the support from NASA which makes these activities possible.

Respectfully submitted,

Carey E. Stronach

Carey E. Stronach
Director
February 14, 1986

200 MeV π^+ Induced Single-Nucleon Removal from ^{24}Mg

Donald Joyce and Herbert O. Funsten
College of William and Mary
Williamsburg, VA 23185

B. Joseph Lieb
George Mason University, Fairfax, VA 22030

Hans S. Plendl and Joseph Norton
Florida State University, Tallahassee, FL 32306

Carey E. Stronach
Virginia State University, Petersburg, VA 23803

V. Gordon Lind, Robert E. McAdams and O. Harry Otteson
Utah State University, Logan, UT 84322

David J. Vieira
Los Alamos National Laboratory, Los Alamos, NM 87545

Anthony J. Buffa
California Polytechnic State University
San Louis Obispo, CA 93401

ABSTRACT

Nuclear γ-rays in coincidence with outgoing pions or protons following single nucleon removal from ^{24}Mg by 200 MeV π^+ have been detected with Ge(Li) detectors. Differential cross sections are reported for γ-rays from the first excited mirror states of ^{23}Na and ^{23}Mg in coincidence with positive pions or protons detected in particle telescopes at 30°, 60°, 90°, 120° and 150°; angle-integrated absolute cross sections and cross section ratios $\sigma(^{23}Mg/\sigma(^{23}Na)$ are calculated. These results are compared with the predictions of a Pauli-blocked plane-wave impulse approximation (PWIA) and the intranuclear cascade (INC) and nucleon charge exchange (NCX) reaction models. The PWIA and the INC calculations generally agree with the angular dependence of the experimental results but not the absolute magnitude. The NCX calculation does not reproduce the observed cross section charge ratios.

PACS number: 25.80 HP

I. INTRODUCTION

The $(\pi,\pi N)$ nuclear reaction offers the potential of a new means of understanding nuclear structure and, at the same time, of studying the propagation of a strong baryon resonance, the Δ, in the nuclear medium. Before this potential can be realized, however, a better understanding of the reaction mechanism must be developed.

The $(\pi,\pi N)$ reaction has been extensively studied using two general types of experiment. In one type of experiment, the residual nucleus or specific states of the residual nucleus are identified through radiochemical techniques [e.g. Ref. 1,2], or via detection of prompt de-excitation γ-rays [e.g. Ref. 3]. Since no kinematical or angular information is obtained, these experiments integrate over both quasifree and non-quasifree components.

Interest in these experiments has centered on the charge dependence of the cross section ratios which were found to differ from the free πN ratios. For example, the cross section ratio $\sigma(\pi^+)/\sigma(\pi^-)$ for π induced neutron removal from ^{12}C was found to have a value of 1/1.7 instead of 1/3 [1].

In the other type of experiment [e.g. Ref. 4,5], the outgoing pion or proton is detected. With the proper geometry, the experimenter can select quasifree events; but only recently has the charged-particle energy resolution become sufficient to identify the final nuclear state. In the work of Kyle et al. [5], the π^+/π^- ratio for proton removal from ^{16}O was found

to be as large as ~40 at forward π angles. They attributed this increase over the free πN value of 9 to a reduction in the $\pi^- p$ quasifree amplitude through destructive interference with another process. They identified the interfering process as ΔN knockout.

The present study includes features of both types of experiment by detecting prompt de-excitation γ-rays in coincidence with the outgoing pions or protons. It thus combines kinematic information with the ability to measure excitation of specific nuclear states.

We studied 200 MeV π^+ incident on a ^{24}Mg target. Outgoing charged particles (scattered π^+ and knocked out protons) were detected by scintillator telescopes at 30°, 60°, 90°, 120° and 150° and identified by their dE/dX. Coincident nuclear γ-rays were detected in one of two Ge(Li) detectors and identified by their energy. One can thus study several different $(\pi,\pi N)$ reaction channels. For example, ^{23}Na γ-rays in coincidence with a π^+ or a p can result only from a direct proton knockout with no charge exchange. ^{23}Mg γ-rays in coincidence with a π^+ can result only from a direct neutron knockout. On the other hand ^{23}Mg γ-rays in coincidence with a proton can only result from a charge exchange reaction.

^{24}Mg was chosen as a target because single nucleon removal from ^{24}Mg results in mirror nuclei ^{23}Mg and ^{23}Na. This provides a test of both single proton and single neutron removal mechanisms with pions. Furthermore, the single nucleon removal spectroscopic strengths ($2d_{5/2}$ and $1p_{1/2}$) for ^{23}Na and ^{23}Mg from

^{24}Mg are concentrated in two low-lying excited states which γ-decay directly to the ground state [6]. For both ^{23}Na and ^{23}Mg, the first excited states ($\approx$0.15 MeV, $5/2^+$) have spectroscopic factors of ~4 to 6, and the $1/2^-$ excited states (at 2.64 MeV in ^{23}Na and at 2.77 MeV in ^{23}Mg) have spectroscopic factors of $\approx$4 as determined from the analysis of single-nucleon removal reactions on ^{24}Mg [6]. This yields for the $5/2^+$ levels an occupation number $C^2S \approx 2$, one-half the $1d_{5/2}$ shell limit of 4 in ^{24}Mg. (C is the isospin coupling coefficient, $(T_f\tau_f|1/2\tau_N|T_i\tau_i) = \sqrt{1/2}$.) Other bound excited states have considerably smaller spectroscopic factors. They predominantly feed the first excited state, but the combined effect of this γ-ray feeding should be less than $\approx$25% of the overall strength of the first excited state (if all states were populated in proportion to their spectroscopic factors).

The suitability of a ^{24}Mg target for $(\pi,\pi N)$ reaction work was established previously by the results of an inclusive study of γ-rays from π^+ reactions on ^{24}Mg [3]. The two above-mentioned states in ^{23}Na and ^{23}Mg with large spectroscopic factors were strongly excited; there was no evidence for background γ-rays that might overlap these states. Another reason for the selection of a ^{24}Mg target was its suitability for a parallel study [7] of the angular correlation of γ-rays from (π,π') scattering.

A feasibility study of the techniques employed in this work was undertaken at LAMPF using a single gamma-ray detector in coincidence with a single charged particle telescope [8]. The

results of that study suggested the need to develop a large-scale coincidence measurement system sensitive to de-excitation gamma rays, knockout nucleons and scattered pions. Such an improved system was developed and used in the present work.

II. EXPERIMENTAL APPARATUS AND PROCEDURES

The experiment was performed with a 200 MeV π^+ beam from the high-energy pion channel (P^3) of LAMPF. This beam had a contamination of 6.6% μ^+ and 2.0% e^+ as well as a muon halo of roughly three times the beam diameter. The beam spot size was typically 2.5 cm in diameter, and the momentum resolution was ≈0.5%. The target consisted of natural magnesium metal (79% ^{24}Mg) with an average density of 0.57 ± 0.02 g/cm^2.

The experimental geometry was defined by six scintillation telescopes for charged particle detection and two Ge(Li) spectrometers to detect γ-rays (see Fig. 1). Each of the six particle telescopes consisted of the six NE 102 scintillators (Ω,Δ,E, rear, left-side veto, and right-side veto). Each scintillator was coupled to a 5 cm photomultiplier tube, except for the E scintillator, which was coupled to two 12.5 cm photomultiplier tubes, one at each end. The detector thicknesses were 0.160 cm (Ω), 0.320 cm (Δ), 0.635 cm (vetos and rear scintillators) and 15.75 cm (E). The dimensions of each telescope component were the same for each telescope with the exception of the Ω scintillators. The Ω scintillators for telescopes 1, 5 and 6 at ± 30° and 150° had to be moved further from the target to avoid the beam halo; they were made correspondingly larger so that all the telescopes subtended the same solid angle.

The Ω and Δ counters together defined the solid angle (~0.18 sr) of each telescope, and the E scintillator determined the

particle energy. All three scintillators were used for particles identification. The rear scintillator tagged particles which had not stopped in the previous scintillators. The two side veto scintillators tagged particles scattering out of or into sides of the E scintillators. During off-line data analysis, however, this feature was not used. Calculation of the telescope solid angles was performed following the method of Gotch and Yogi [9], considering the size and location of the Ω, Δ and E scintillators for each telescope. All telescopes except number 6 were mounted together on a pivoting table with their axis directly under the target centerline. Telescope 6 was mounted on a similar but smaller table pivoting on the same axis.

Two Ge(Li) γ-ray spectrometers were used in the present experiment, an Ortec 9% efficient and a Princeton Gamma-Tech 11% efficient lithium drifted germanium detector. Both detectors were fitted with NE 102 anti-coincidence scintillators cups to tag charged particles entering them. They were mounted on one rolling table to facilitate positioning and shielding. One detector was located at -75° and the other at -122° relative to the pion beam line axis (see Fig. 1). Additional experimental details are given in Ref. [7].

The beam intensity was monitored with a 7.6 cm thick ion chamber filled with argon, and the beam profile was monitored with a LAMPF wire chamber system [10]. The absolute cross sections were normalized to the differential inelastic π scattering cross sections from the 2^+ state of ^{24}Mg [11].

The six telescopes were calibrated in energy by tuning the channel for low-intensity protons at 50 MeV, 133 MeV and 191 MeV and placing each of the telescopes in the beam. The telescopes were also calibrated with the pion and proton quasi-elastic scattering peaks from the experimental runs as well as with the maximum energy deposited in the E scintillators for pions and protons. The telescope calibration runs were also used to determine the efficiencies of the six telescopes. They were found to average 96 ± 2%.

The energy responses of the two Ge(Li) detectors were periodically calibrated by placing ^{228}Th, ^{54}Mn and ^{137}Cs sources at the target location. Well-known strong γ-ray peaks in the experimental data provided additional energy calibration, including the ^{24}Mg first excited state to ground transition and the ^{23}Na first excited state to ground transition. The maximum deviation of the calibration data from a linear fit was 0.7 keV. Relative and absolute Ge(Li) detector efficiencies were also determined in the source calibration runs.

A valid data event consisted of a coincidence between a particle telescope signal and a Ge(Li) γ-ray. For each event, pulse heights were digitized for Ω, Δ, E (two photomultipliers), and rear scintillators as well as the Ge(Li) detectors. All data were read into a PDP-11 computer and written on magnetic tape for later replay.

Particles were identified from their Δ and E pulse heights using the method of Goulding et al. [12]. A particle which

passed completely through the E scintillator (75 MeV pions) and 160 MeV protons) as indicated by the rear scintillator was treated using the method of England [13]. Figure 2 shows a typical dE/dx vs. E dot plot (for Telescope 1, 30°), with the pions and protons identified.

During off-line data analysis, spectra were accumulated for γ-rays in one of the two Ge(Li) detectors that were in coincidence with pions or protons in any one of the six particle telescopes. Statistics were not sufficient to allow meaningful cuts on pion or proton energy. Figure 3 shows the spectrum in the Ge(Li) detector at 75° in coincidence with a pion or a proton in any one of the six telescopes. Figure 4 shows the random (off timing peak) spectrum for this detector.

The γ-rays in these spectra were identified by their energy, and areas were determined by summing channels and subtracting background. Cross sections were calculated from the relative areas and from the Ge(Li) and the particle telescope efficiencies. As noted above, the cross sections were normalized to the ^{24}Mg 2^+ differential inelastic scattering cross sections of Bolger [11]. Major sources of error were the following: statistical errors, errors in the absolute normalization to the inelastic data (≈15%), Ge(Li) efficiency calibration (≈9%), and telescope solid angle determination (≈6%).

In addition to the strong first excited $t/2^+$ states at 0.439 MeV in ^{23}Na and 0.450 MeV in ^{23}Mg (see Fig. 3), there was evidence for the fourth excited $1/2^-$ state in ^{23}Na at 2.64 MeV;

but its Doppler-broadened width prevented a differential cross section measurement. There was no sign of its mirror state in ^{23}Mg.

III. COMPARISON OF ANGULAR DISTRIBUTIONS WITH REACTION MODELS

The experimental differential cross sections for production of the 0.439 and 0.450 MeV γ-rays in coincidence with outgoing pions or protons are listed in Table I for the two Ge(Li) detectors. The averages (last column of Table I) were calculated using the inverse of the fractional errors as weights. Where two cross sections differed greatly, the errors were increased in order to be more conservative. Data from Telescopes 1 and 6 were averaged to give one data point at 30°.

The cross sections were extracted from the data by assuming isotropic γ-ray correlation with the outgoing pion or proton. This assumption would be rigorously true for direct plan wave nucleon knockout and can be seen to be approximately true within experimental uncertainties by comparing the relative cross sections of Ge(Li) 1 and 2 listed in Columns 4 and 5 of Table I. (Ge(Li) 1 and 2 had an angular separation of 50°.) This absence of angular correlation is in contrast to the expected strong $\sin^2 2\theta_{\gamma q}$ correlation that was observed in this experiment for inelastic π^+ scattering to the 1.37 MeV first excited state of ^{24}Mg [7]. ($\theta_{\gamma q}$ is the angle between the γ-ray and the inelastic momentum transfer direction.)

Proton and pion differential cross sections were compared with predictions of an intranuclear cascade (INC) code developed by Frankel et al. [14] and with the predictions of a simple plane-wave impulse approximation (PWIA) which assumes only a

single collision of the incident pion with a nucleon. In Section IV, cross section charge ratios are compared with these models and also with a model that assumes final-state nucleon charge exchange (NCX) [15].

The INC predictions were based on $5 \cdot 10^4$ cascades of 200 MeV π^+ on ^{24}Mg. The program output was sorted to yield differential π^+ and proton cross sections at the angles measured in the present experiment for events in which the final nucleus was ^{23}Na or ^{23}Mg in a bound state. In performing these calculations, that part of the code that evaluates evaporation subsequent to the cascade was not used. Instead, a ^{23}Na or ^{23}Mg nucleus was assumed to retain its identity if its excitation energy calculated by INC following the cascade was less than its known particle stability energy. (The INC code does not include details of nuclear structure or predict specific nuclear states. It has, hwoever, no free parameters.) Since the INC-calculated contributions to the $^{23}Na/^{23}Mg$ bound states arose from the entire nuclear volume and not just from the nuclear surface (i.e. $1d_{5/2}$ shell nucleons), one should multiply the INC results by the ratio $r = \Sigma_p S^-(J^P) \cdot F(J^P, 5/2^+)/\Sigma_p S^-(J^P)$, where $S^-(J^P)$ is the spectroscopic factor for neutron or proton removal to a ^{23}Na or ^{23}Mg bound state of spin parity J^P and $F(J^P, 5/2^+)$ is the relative fraction of γ feeding from an initial J^P state down to the $5/2^+$ first excited state. Using spectroscopic factors and γ branching ratios from ref. [6], $r \doteq 0.6$ for both ^{23}Na and ^{23}Mg. The INC

results quoted in the present paper have been reduced by this factor.

Analysis of the output from the INC calculation showed that a large fraction (≈90%) of production of a bound a state of the A-1 residual nuclei results from a single collision of the incident pion pion on a nucleon with no further interaction. The probability of the residual nucleus being left with a given excitation decreases monotonically with increasing excitation energy.

The PWIA predictions for the cross sections were calculated using the semiempirical free πN phase shift of Rowe et al. [16]. The resulting cross sections were reduced, at small pion scattering angles, by Pauli blocking using a degenerate Fermi sphere uniformly filled up to a momentum of k_F = 270 MeV/c. The Pauli blocking was calculated from the quantity (V-N)/V, where N is the phase space volume common to the Fermi sphere and a similar Fermi sphere whose center is displaced by an amount $q = 2k_\pi \sin \theta_\pi/2$, and V is the sphere's volume. This caused the resulting cross section at $\theta_\pi = 0°$ to be 0 and at θ_π - 80° to approach the free π-N cross section. This cross section was then multiplied by the $1d_{5/2}$ proton or neutron occupation number for the first excited state, $C^2S^-_N = 2.2$ defined above. It was necessary to additionally scale the resulting PWIA prediction to the data by multiplying by factors of ~1/3 to 1/5. This indicates the predominance of other processes such as pion absorption and secondary scatterings.

The PWIA calculation was performed only to estimate the trends of the experimental data. It, however, demonstrates the role of Pauli blocking in reducing the forward angle pion scattering from the free πN.

A. Pion angular distributions

Figure 5 shows experimental and calculated angular distributions for outgoing pions that are in coincidence with γ rays from the first excited states of ^{23}Mg and ^{23}Na. The solid curve represents the Pauli-blocked PWIA results described above; the open circles are the results from the INC calculation. Without Pauli blocking, the pion differential cross section would rise steadily as θ decreases below ~60°. At θ_π = 30°, the PWIA cross section is reduced by a factor of ~2 relative to the free case. Both INC and PWIA calculations (and the data) display Pauli blocking with decreasing θ; the INC cross section falls off more rapidly than the PWIA cross section. An effect that could account for this discrepancy is nuclear shadowing of forward-scattered pions for the INC calculation. In the PWIA calculation, this effect has not been included.

B. Proton angular distributions

Figure 6 displays the experimental angular distributions for outgoing protons in coincidence with γ-rays from the first excited states of ^{23}Mg and ^{23}Na, together with PWIA and INC results (solid curves and open circles, respectively). The

angular distributions have the general shape of free π-N scattering, in which case no protons would be emitted at angles greater than 90°.

The E scintillator thickness (15 gm/cm^2) was insufficient to permit derivation of pion energy spectra but was adequate for determination of proton energy spectra by use of a fold-back procedure [7]. The 30° and 60° γ-coincident proton spectra are shown in Fig. 7. The arrows indicate the energies for free πN scattering; the dashed lines indicate the INC results. Coincident proton spectra for $\theta_p \geq 90°$ had few total counts; as expected, no peak was observed. The apparent differences between the 60° spectra and the INC predictions may be instrumental: the steep left-hand shoulder is due to electronic low-energy cutoff, and the high-energy tail is partially due to scintillator energy resolution. The cross sections at 60° were corrected for the low-energy cutoff.

IV. ABSOLUTE CROSS SECTIONS

Table II compares experimental and calculated angle-integrated absolute cross sections. It shows that the observed cross sections are ~1/3 to ~1/5 of those predicted by the PWIA but are 3 times those predicted by INC. Particularly at the Δ resonance energy, the assumption of a single πN interaction which is implicit in the PWIA is questionable. The 200 mb free πN cross section at the resonance yields a spatial width of ~5f resulting in a "swelling" of the nucleon to a size encompassing up to two adjacent nucleons. This "swelling" yields total π-nucleus cross sections that are typically twice the nuclear geometrical cross section. For example, in ^{27}Al, the geometrical cross section is ~450 mb whereas the total pion cross section is ~960 mb [16] and is divided approximately equally among pion capture, nuclear elastic and non-elastic processes. The cross sections that remain for production of states observed in the present experiment are thus a small fraction of the total cross sections and would be sensitive to variations in any of the above components.

The ratios $\sigma_\pi(^{23}\text{Na})/\sigma_p(^{23}\text{Mg})$ for the π^+ coincident differential cross sections have values of ~4, approximately independent of θ_π (see Table 1). This is in disagreement with the results of Kyle et al. [5] at T_π = 240 MeV in which the corresponding charge ratio $R = \sigma(\pi^+)/\sigma(\pi^-)$ for $^{16}\text{O}(\pi^\pm,\pi^\pm\text{p})^{15}\text{N}_{\text{g.s.}}$ reaches a very large value, $R \geq 30$, for forward angles, $\theta_\pi \leq 35°$. Kyle et

al. suggests that this enhancement over the quasifree value of 9 comes from a reduction in the π^-p cross section, as π^+p enhancement is unlikely. In our experiment, however, the angle-integrated π^+ coincident ^{23}Mg $5/2^+$ cross section, which corresponds to the π^- cross section of Kyle et al., is relative to PWIA, the largest of all four measured cross sections (see Table II, column 7). It may be noted that the enhancement found by Kyle et al. occurs at scattering angles where Pauli blocking is predominant.

Our π^+ and p coincident ^{23}Na cross sections are in agreement with equivalent cross sections obtained from $^{12}C(\pi^+,\pi^+p)$ data of Piasetzky et al. [4] who used a double arm spectrometer system. Their cross section values approximately equal those for free π^+p scattering; and assuming that four p shell protons are available, their effective participation ratio is approximately 0.25, which agrees with our results for ^{23}Na (Table II, column 7). However, their $^{12}C(\pi^-,\pi^-p)$ cross section is ~60% greater than our equivalent π^+ coincident ^{23}Mg cross section.

The INC predictions as mentioned above fall below the experimental results by a factor of ≈1/3. An examination of the particle histories generated by the INC code yields the following further information on the $^{24}Mg(\pi,\pi p)$ reaction:

A. INC predicts total, elastic, and absorption cross sections of 980, 400, and 230 mb, respectively, in

general agreement with 960, 380 and 218 mb, respectively, as measured by Ashery et al. [17] for 245 MeV $\pi^+ + {}^{27}Al$.

B. INC indicates that 75% of the Δ's decay before striking a nucleon. This is due to the short free decay length of the Δ (~0.4 f). Our PWIA calculation indicates that Pauli blocking of the decay is not predominant - only ~1/3 of the Δ decays are Pauli-blocked.

C. According to the INC results, pions from Δ decay predominately do not escape the nucleus; 75% of the pions from Δ decay strike a nucleon to re-form another Δ. Using the Δ decay probability given above in B, this yields an average of two sequential Δ's formed for each T = 200 MeV pion incident on the nucleus. In a single scattering, the pion loses an average of 60 MeV lab kinetic energy; after two or more pion scatterings through Δ formation, T_π will have dropped considerably below resonance energy. INC yields a pion scattering mean free path λ_π of 1.2 f; cf. $\lambda_\pi = 1/\rho\sigma_\pi$ total $\doteq$ 2.3 f. (Pion absorption occurs only through $\Delta N \rightarrow NN$).

D. INC indicates that approximately 70% of the protons resulting from Δ decay escape the nucleus without further scattering. INC yields λ_p = 4.5 f; this in agreement with $\lambda_p = 1/\rho\sigma_p$ > 5 f obtained from free, but Pauli blocked [18] NN total cross sections [19] and a ^{24}Mg uniform nuclear matter density ρ of radius 1.315 f

[20]. The INC result is also in agreement with estiamtes by Schiffer [21]. Of the scattered Δ decay protons, approximately half undergo charge exchange before escaping in the INC calcualtions. Since only 30% of the protons do not escape, this yields a probability for NCX of ≈15%.

E. Approximately 40% of the total cross section for incident pions results in pion capture (ΔN→NN), according to the INC calculation. Measurements by Ashery et al. [17] indicate a ratio of capture-to-total cross section of ≈30%.

In a recent paper, Frankel et al. [22] explored the effects of using a different nucleon momentum distribution in the INC code. The usual version (the one used in the present paper) assumes a local, degenerate Fermi gas distribution. This was changed to a shell model with harmonic oscillator wave functions. The latter momentum distribution improved the INC code agreement with the $(\pi,\pi p)$ angular correlation data of Piasetzky et al. [4]. Since the π^- induced nucleon removal is likely to be a surface reaction, the use of a more realistic momentum distribution could improve agreement with the present results.

The INC results discussed above suggest that pion multiple scattering, occurring mainly by sequential Δ production and decay, is a predominant process, being more important (λ_π = 1.2 f) than nucleon multiple scattering ($\lambda_p \approx 5$ f) which

was proposed some time ago [15] as a major process in pion-induced nucleon knockout at Δ resonance energies. In the latter process the nucleon from Δ decay undergoes subsequent incoherent nuclear scattering with a probability of nucleon charge exchange (NCX), $P \doteq 0.1 \rightarrow 0.2$ [15] as determined from cross section ratios obtained in $\sigma[^{12}C(\pi^+,X)^{11}C]/\sigma[^{12}C(\pi^-,X)^{11}C]$ activation experiments [1]. In the present experiment, both π^+ and p coincident cross sections for de-excitation γ-rays are determined. Hence the present experiment provides a more sensitive test of the NCX model than the previous activation experiments, which sum over these two final states.

The NCX calculation predicts cross sections for the final states $^{23}Mg + \pi^+$, $^{23}Mg + p$, $^{23}Na + \pi^+$, and $^{23}Na + p$ to be in the ratio of (1+9P):2:(9+P):(9+P). Since the ^{23}Na residual nucleus must be accompanied by both π^+ and p, the final states $^{23}Na + \pi^+$ and ^{23}Na +p must have the same cross sections regardless of the reaction model. Hence, the two experimental ^{23}Na cross sections (see Table II) were averaged, yielding $\sigma[^{23}Na(Av)] = 48 \pm 8$ mb. There are then only two independent cross section ratios. Let them be the ratios of $\sigma[^{23}Mg+\pi^+]$ and $\sigma[^{23}Mg+p]$ to $\sigma[^{23}Na(Av)]$. The first ratio,

$$R_1 = \sigma[^{23}Mg + \pi^+]/\sigma[^{23}Na(Av)] = .23 \pm .04,$$

yields $P \approx .12 \pm .04$, consistent with values of P obtained from activation work. (Quasifree $R_1 = 1/9$). However, the second

ratio, obtained from the proton component of the ^{23}Mg final state, has a value

$$R_2 = \sigma[^{23}Mg + p]/\sigma[^{23}Na(Av)] \approx .33 \pm .05,$$

yielding a negative value of P, $P = -2.9 \pm .9$, which is inconsistent with NCX, even though the uncertainty is quite large. (Quasifree $R_2 = 2/9$). Because of electronic cutoff and the lack of scintillators in the forward direction where the proton cross section peaks, we may be undercounting proton events and hence R_2. However, increase in R_2 would worsen agreement with NCX.

A comparison of our experimental results with the results of activation measurements can be made by summing the measured π^+ and p components of the ^{23}Mg cross section (see Table II). This yields a ratio of

$$\sigma[(^{23}Mg + \pi^+)+(^{23}Mg + p)]/\sigma[^{23}Na(Av)] \approx .56 \pm .06,$$

which in turn yields a value of $P \approx .24 \pm 0.07$, consistent with the value of P obtained from activation measurements.

The above results indicate that whereas the NCX model can explain inclusive cross section results like those obtained by activation measurements, it is inconsistent with the more exclusive cross sections obtained in the present experiment. In a recent paper, Ohkubo and Liu [23] include the effects of quantum mechanical interference between quasifree and non-quasifree (NCX and π charge exchange) reaction processes using distorted waves. Their calculations result in significantly

better agreement with the experimental results for $^{22}C(\pi^+,\pi N)^{11}C$ cross section ratios [1] than the previously incoherent NCX calculations [15]. In a subsequent paper Ohkubo, Liu et al. [2] conclude that both NCX and the interference effects decrease considerably in magnitude as the target mass is increased from A = 12. Their results suggest that these effects are small for an A = 24 target.

A process in which an initial Δ subsequently interacts with a nucleon in a $(\Delta N)^{T=2}$ state can, by itself, reproduce measured values of R_1 and R_2. Such a process, in which one of the $(\Delta N)^{T=2}$ decay nucleons subsequently remains in the nucleus, yields $R_1 = 0.22$, $R_2 = 0.37$, i.e. values close to those observed. Although there has been evidence for a possible $(\Delta N)^{T=2}$ attractive potential [24], an examination of the magnitude of pion double charge exchange cross sections casts doubt on this process. Even after allowing for the isospin recoupling, which yields for pion double charge exchange a $(\Delta N)^{T=2}$ component -1/3, any ΔN contribution that is sufficiently large to yield a reasonable $(\pi,\pi N)$ reaction would result in a pion double charge exchange cross section too high by at least a factor of 10.

V. CONCLUSION

The experimentally determined pion and proton differential cross sections for de-excitation γ-rays from the $5/2^+$ first excited states of ^{23}Na and ^{23}Mg in coincidence with outgoing π^+ or p from $^{24}Mg(\pi^+,\pi N)$ have been measured and compared with the results of calculations based on several $(\pi,\pi N)$ reaction models, in particular on a Pauli blocked plane-wave impulse approximation (PWIA), on intranuclear cascade (INC) models, and on charge exchange of the outgoing nucleon (NCX).

Both the PWIA and the INC calculations reproduce the approximate shape of the observed π^+ and p angular distributions, but not the magnitude. The PWIA calculation, which was done primarily to illustrate the trends in the data, resulted in cross sections that were a factor of ~3 to 5 too large. On the other hand, the INC calculations, which can be considered absolute, were a factor of ~3 too small. These calculations indicate that rescattering of the outgoing pions is a more important process than interaction of the outgoing nucleons. The NCX model is put to a more sensitive test by the present experiment than by previous activation experiments, since π^+ and p coincident cross section ratios for de-excitation γ-rays are determined separately rather than together. The NCX results are inconsistent with experimental results.

These comparisons with several reaction models suggest that a more detailed description of the πN interaction in a nucleus,

such as the Δ-hole model of Hirata, Lenz and Thies [25], may be needed for a better understanding of the processes involved in the $(\pi,\pi N)$ reaction.

ACKNOWLEDGEMENTS

We wish to thank Jean Julien, Herbert O. Funsten, III and David C. Plendl for their participation in the data collection, Peter Gram for valuable discussion on experimental details, and Robert Damjanovich and other members of the LAMPF staff for technical assistance. This work was supported in part by the NSF; the participation of one of us (C.E.S.) was also supported in part by NASA.

REFERENCES

1. B. J. Dropesky, G. W. Butler, C. J. Orth, R. A. Williams, M. A. Yates-Williams, G. Friedlander and S. B. Kaufman, Phys. Rev. C20, 1844 (1979).

L. H. Batist, V. D. Vitman, V. P. Koptev, M. M. Makarov, A. A. Naberezhnov, V. V. Nelyubin, G. Z. Obrant, V. V. Sarantsev and G. V. Scherbakov, Nucl. Phys. A254, 480 (1975).

2. Y. Ohkubo, C. J. Orth, D. J. Vieira and L. C. Liu, Phys. Rev. C31, 510 (1985).

3. B. J. Lieb, H. S. Plendl, C. E. Stronach, H. O. Funsten and V. G. Lind, Phys. Rev. C19, 2405 (1979).

4. E. Piasetzky, D. Ashery, A. Altman, A. J. Yavin, F. W. Schleputz, R. J. Powers, W. Bertl, L. FElawka, H. K. Walter, R. G. Winter and J. Van Der Pluym, Phys. Rev. C25, 2687 (1982).

5. G. S. Kyle, P. A. Amandruz, Th. S. Bauer, J. J. Domingo, C. H. Q. Ingram, J. Jansen, D. Renker, J. Zichy, R. Stamminger and F. Vogler, Phys. Rev. Lett. 52, 974 (1984).

6. P. M. Endt and C. Van der Leun, Nucl. Phys. A310, (1978).

7. D. Joyce, Positive Pion Scattering on ^{24}Mg. Ph.D. Thesis, College of William and Mary (1982).

8. V. G. Lind, R. E. McAdams, O. H. Otteson, W. F. Denig, C. A. Goulding, M. Greenfield, H. S. Plendl, B. J. Lieb, C. E. Stronach, P. A. M. Gram and T. Sharma, Phys. Rev. Lett. 11, 1023 (1978).

9. H. Gotch and H. Yogi, Nucl. Inst. Methods 96, 185 (1971).

10. G. J. Krause and P. A. M. Gram, Beam Profile Monitor, LASL Report LA-7142 (1978).

11. J. Bolger, private communication (1979).

12. F. S. Goulding, D. A. Landis, J. Cerny and R. H. Pehl, Nucl. Inst. Methods 31, 1 (1964).

13. J. B. A. England, Techniques in Nuclear Structure Physics Part 2, p. 419, John Wiley and Sons (1974).

14. Z. Frankel, Phys. Rev. 130, 2407 (1963).
G. D. Harp, K. Chen, G. Friedlander, Z. Frankel and J. M. Miller, Phys. REv. C8, 581 (1973).

15. M. M. Sternheim and R. R. Silbar, Phys. Rev. Lett. 34, 824 (1975).

16. G. Rowe, M. Salomon and R. H. Landau, Phys. Rev. C18, 584 (1978).

17. D. Ashery, I. Navon, G. Azuelos, H. J. Pfeiffer, H. K. Walter and F. W. Schleputz, Phys. Rev. C23, 2173 (1981).

18. K. Nishijima, Fundamental Particles, p. 98, W. J. Benjamin (1963).

19. W. N. Hess, Rev. Mod. Phys. 30, 368 (1968).

20. Landolt and Bornstein, Nuclear Radii (Springer-Verlag, Berlin, 1967), Vol. 2.

21. J. P. Schiffer, Nucl. Phys. A335, 339 (1980).

22. Z. Fraenkel, E. Piasetzky and G. Kalbermann, Phys. Rev. C26, 1618 (1982).

23. Y. Ohkubo and L. C. Liu, Phys. Rev. C30, 254 (1984).

24. H. Toki, private communication.

25. M. Hirata, F. Lenz and M. Thies, Phys. Rev. C28, 785 (1983).

FIGURE CAPTIONS

1. Experimental Geometry. The rear and side veto counters surrounding each E counter are shown but not labeled.
2. A dE/dx vs. E dot plot for telescope 1 at 30°. The E signal was from one of the two photomultipliers of that scintillator.
3. Ge(Li) #1 γ-ray spectrum in coincidence with a π^+ or p from $^{24}Mg(\pi^+,\pi N)$ in any one of the six particle telescopes (low-energy portion).
4. Ge(Li) #1 γ-ray spectrum in random coincidence (low-energy portion).
5. Differential cross sections of outgoing π^+ from $^{24}Mg(\pi^+,\pi^+N)$ in coincidence with γ-rays from the first excited states of ^{23}Na and ^{23}Mg compared with Pauli-blocked plane-wave impulse approximation (PWIA) and intranuclear cascade (INC) calculations. PWIA values have been multiplied by 0.20 for ^{23}Na and by 0.38 for ^{23}Mg.
6. Differential cross sections of protons from $^{24}Mg(\pi^+,\rho p)$ in coincidence with γ-rays from the first excited states of ^{23}Na and ^{23}Mg compared with Pauli-blocked plane-wave impulse (PWIA) and intranuclear cascade (INC) calculations. PWIA values have been multiplied by 0.17 for ^{23}Na and by 0.28 for ^{23}Mg. PWIA and INC values at backward angles are <0.1 mb/sr and hence do not show up on the semi-log plot.

7. Energy spectra of protons from $^{24}Mg(\pi^+,p)$ detected at 30° and 60° in coincidence with γ-rays from the first excited states of ^{23}Na and ^{23}Mg compared with INC calculations (dashed line). The arrows indicate the energies for free πN scattering.

Table I

Experimental differential cross sections for $^{24}Mg(\pi,\pi N)$.

$\sigma_\pi(^{23}Na)$ is the differential cross section for production of the ^{23}Na first excited state ($5/2^+$, 0.439 MeV) in coincidence with a π^+. Similar definitions apply for the other cross sections. Results are shown for each Ge(Li) and as an average which was weighted by the fractional errors. Telescope 1 was averaged with Telescope 6 for the 30° results.

Reaction	Telescope	Angle	Ge(Li)1 $\frac{mb}{sr}$	Ge(Li)2 $\frac{mb}{sr}$	Average $\frac{mb}{sr}$
$\sigma_\pi(^{23}Na)$	1	30°	7.3±1.9	4.6±1.2	5.2±1.1
	6	30°	4.8±1.3	1.9±1.3	
	2	60°	4.4±1.2	3.3±0.9	3.9±0.9
	3	90°	4.0±1.1	1.6±0.5	3.0±1.0
	4	120°	6.3±1.7	4.1±1.1	5.2±1.0
	5	150°	6.2±1.6	4.2±1.1	5.2±1.0
$\sigma_\pi(^{23}Mg)$	1	30°	1.5±0.5	1.9±0.5	1.4±0.5
	6	30°	1.4±0.5	0.31±0.15	
	2	60°	1.1±0.4	0.74±0.25	0.90±0.22
	3	90°	0.82±0.34	0.97±0.30	0.92±0.23
	4	120°	1.2±0.5	0.89±0.29	1.0±0.25
	5	150°	0.72±0.28	1.3±0.4	1.1±0.30
$\sigma_p(^{23}Na)$	1	30°	15.0±4.0	16.0±4.0	15.0±4.0
	6	30°	18.0±4.0	11.0±3.0	
	2	60°	4.8±1.3	4.0±1.1	4.4±0.9
	3	90°	0.59±0.28	0.85±0.30	0.76±0.20
	4	120°	1.5±0.5	0.87±0.31	1.2±0.3
	5	150°	1.3±0.5	0.45±0.20	0.93±0.27
$\sigma_p(^{23}Na)$	1	30°	7.6±2.0	7.7±1.9	5.8±1.4
	6	30°	5.1±1.4	2.8±0.80	
	2	60°	2.1±0.7	1.3±0.4	1.7±0.4
	3	90°	0.48±0.24	0.31±0.15	0.39±0.14
	4	120°	0.45±0.25	0.59±0.25	0.54±0.18
	5	150°	0.93±0.38	0.28±0.15	0.69±0.22

NPL-996

$^4He(\vec{p},d)^3He$ Reaction at 200 and 400 MeV

P. W. F. Alons, J. J. Kraushaar, and J. R. Shepard
Nuclear Physics Laboratory, Department of Physics, University of Colorado
Boulder, CO 80309, USA

J. M. Cameron, D. A. Hutcheon, R. P. Liljestrand*
W. J. McDonald, C. A. Miller and W. C. Olsen
Department of Physics, University of Alberta
Edmonton, Alberta, Canada T6G 2N5

J. R. Tinsley**
Department of Physics, University of Oregon,
Eugene, OR 97403, USA

C. E. Stronach
Department of Physics, Virginia State University
Petersburg, VA 23803, USA

PAC Index 25.40 Gr

I. INTRODUCTION

The $^4He(p,d)^3He$ reaction possesses some appealing theoretical features. The nuclear structure involved is relatively simple since essentially only 1S orbitals can participate. Furthermore, the wavefunctions can be constrained by the wealth of experimental information on ^3He and ^4He. This permits investigation of the reaction mechanism with a minimum of additional theoretical uncertainties. In particular, one may be able to learn about the role of pion emission and absorption processes as well as intermediate Δ formation in the (p,d) process. For such light systems exchange processes, in this case the two nucleon pick-up process $^4He(p,^3He)^2H$, may also be important. In addition, knowledge of the cross sections over a wide energy range is useful in astrophysical calculations of the production of ^3He. While there have been several studies at proton energies less than 100 MeV, there are very few published data at higher energies where there is a large momentum transfer. In addition, analyzing power measurements, which are most important in trying to assess the validity of the reaction mechanism being used, have only been taken at 32 and 50 MeV, although some unpublished data exist at 650 and 800 MeV.[1] In order to provide additional intermediate energy data on this reaction, the present measurements have been made at TRIUMF using the 1.4 GeV/c spectrometer and beams of polarized protons of 200 and 400 MeV.

Although the details of the reaction mechanism appropriate for the (p,d) reaction on a very light target at an energy of several hundred MeV are not entirely clear, the data to be presented will be compared to exact-finite-range distorted wave calculations using the adiabatic approximation for the deuteron potential. These calculations will at least serve as a reference frame for discussing additional aspects of the

reaction mechanism that should be included in the calculations. In order to provide a consistent set of energy dependent optical potential parameters for the proton channel, proton - ^{4}He elastic scattering data from 85 to 800 MeV were fitted using a search procedure. Distorted-wave calculations were carried out and comparisons were made with existing data at 156 MeV[2] and 770 MeV[3] as well as with the data presented in this paper.

II EXPERIMENTAL PROCEDURES

A polarized proton beam from the TRIUMF cyclotron was used in conjunction with the 1.4 GeV/c magnet spectrometer (MRS) and a liquid ^{4}He target to carry out the measurements. Details of the apparatus and the method used in determining the polarization of the beam[4-6] and the construction of the liquid ^{4}He target [7,8] have been published previously. The polarization of the beam was typically 60 to 70% and was monitored continuously during a run by a polarimeter and a thin CH_2 foil that was inserted in the beam. The beam polarization was known to ±0.03. The liquid ^{4}He was about 33 mg/cm^2 thick and was contained in a cell that had separate Kapton and nickel windows that were 0.15 mg/cm^2 thick.

The essential features of the magnetic spectrometer that are relevant to the present experiment have also been described previously.[9] The momentum acceptance of the spectrometer was set at about ±7%. Deuteron spectra at 200 and 400 MeV taken during the measurements have been published[10] and the deuteron group to the ground state of ^{3}He is well resolved from the continuum with little background contribution.

Normalization of the cross sections was based on elastic ^{4}He(p,p) data, which were taken at 200 MeV at scattering angles of 16, 30 and 45° and compared to the published cross sections of Moss et al.[11] It is estimated that the uncertainty in the absolute values of the cross sections

is no larger than 20%.

The cross sections at 200 and 400 MeV are displayed in Fig. 1 and the analyzing power data in Fig. 2; the numerical values are shown in Table I. The error bars shown on these data are based on statistics only. Also shown in Fig. 1 as the open circles are the back angle cross section measurements of Cameron et al.[12] at 400 MeV.

III DISTORTED WAVE CALCULATIONS

In order to provide optical model parameters for the incident protons in the DWBA calculations, a series of parameter searches were carried out with proton elastic scattering data on ^{4}He that ranged in energy from 85 to 800 MeV. Explicitly elastic cross section and analyzing power data at 85 MeV,[13] 200, 350 and 500 MeV,[11] and 800 MeV[14] were used with the search program MAGALI,[15] which was extended to include relativistic kinematics. In the search procedure the values of r_R and a_R, the radius and diffuseness parameter of the real potential, were fixed at 1.244 and 0.206 fm, and a_I, the diffuseness parameter for the imaginary volume potential, was fixed at 0.336 fm. With these restraints optimum values for V_R, W_I, r_I, V_{so}, r_{so}, and a_{so} were obtained for the elastic data at the five energies. In this way curves could be constructed for these parameters that varied smoothly in energy. The proton parameters at the four energies of interest for the (p,d) reaction were then taken from these plots and their values are shown in Table II.

The deuteron optical potentials used were based on the adiabatic deuteron approximation of Johnson and Soper.[16] This was done in part because very few deuteron - ^{3}He elastic scattering data are available in the energy range of interest but mainly because the adiabatic model compensates for the deuteron break-up effects. The actual deuteron

parameters that were used are shown in Table II and were constructed from the p+^{4}He potential parameters at one half the corresponding deuteron laboratory energy generally following the prescription of Harvey and Johnson,[17] while taking into account that the deuteron scatter from ^{3}He rather than ^{4}He.

For the bound state of the transferred nucleon two form factors were used. The first form factor was a simple Gaussian 1S wave function from a harmonic oscillator well with a harmonic oscillator parameter, b=1.42 fm.[18] This oscillator parameter was obtained by fitting the momentum distribution of protons measured in the ^{4}He(e,e'p) reaction[19] with a Gaussian function.

The second form factor was derived using a procedure derived by Shepard et al.[20] Here the charge form factor obtained from electron-^{4}He elastic scattering data was modified by subtracting pion exchange current contributions to give a true nucleon density. A Fourier transform was then taken of the modified charge density to yield a form factor whose numerical values were directly used in DWUCK5.[21] This exact-finite-range program allows for the inclusion of non-local effects by the introduction of a non-locality parameter, β. The values that were used at all energies were 0.85 for the incoming proton and 0.54 for the outgoing deuteron. Calculations were also carried out for both form factors with the non-local parameter set equal to zero. In the calculations shown a spectroscopic factor of 2 has been assumed and is included in the calculations.

IV Conclusions

The comparison of the distorted wave calculations with the ^{4}He(p,d) cross section data is shown in Figs. 1, 3, and 4. At all four energies the theoretical description of the data is relatively poor. While the general

magnitude of the cross sections is not in bad agreement, the detailed slopes of the theoretical angular distributions miss the shapes of the experimental data in a rather fundamental way. The differences between the calculations carried out with the two different form factors for the bound state calculation are relatively minor except at 770 MeV, where the Gaussian form factor provides far less structure than does the one based on the charge density distribution of ^{4}He.

As shown in Fig. 2, the calculations provide a reasonable description of the analyzing power data. At 400 MeV the description is most encouraging. The results of the calculations with the non-local parameter, β, set equal to zero are not shown in the figures. The effect on the cross sections of having β=0 was negligible. The effect on the analyzing power prediction at 156 and 200 MeV was to reduce rather drastically the magnitudes of A_y. At 400 and 770 MeV the effect was to change completely the angular dependence such as to destroy any agreement with the 400 MeV data.

It is clear that the pickup reaction mechanism that has been assumed is in general not accounting for the data in an adequate fashion. Apart from the direct one nucleon transfer process there are additional processes that may contribute to the ^{4}He(p,d) cross sections. Some of these are presented by the diagrams in Fig. 5. Figure 5a pictures the direct one nucleon transfer assumed in the DWBA calculations presented. Figure 5b represents the "heavy particle stripping" contributions, which involve here a direct two nucleon transfer. This coherent contribution is certainly expected to be more important here than for the case of a (p,d) reaction on heavier nuclei, where the heavy particle stripping involves the transfer of a (much) larger nuclear cluster. Calculations that include this exchange

contribution are being pursued. The rise in the cross sections at scattering angles greater than about 100° is clearly seen in the 156 MeV data and in the 400 MeV data between 160 and 180°. This is no doubt mainly due to the two nucleon transfer. In fact plane wave calculations carried out by Bernas et al.[2] account for this general back angle rise in the cross sections in terms of this process. In a similar fashion, two-nucleon transfer calculations were carried out to account for the large angle (p,d) data taken at a proton energy of 85 MeV. It will be important to see the results for even the forward angle region when the one and two nucleon transfer contributions are added coherently.

Figures 5c and 5d represent processes in which the momentum transfer is shared between two nucleons, one nucleon becoming a delta. These processes may be expected to give substantial contributions at higher energies, because of the momentum mismatch which is especially important for ℓ=0 transitions. Calculations of the general type indicated in diagram 5(c) were carried out by A. Boudard et al.[22] for the $^{16}O(d,p)^{17}O$ reaction at E_d=698 MeV. Here the one-nucleon stripping cross sections alone overpredicted the measured cross sections by a factor of about 7. Inclusion of double pion rescattering with intermediate Δ excitation had the general effect of reducing the predicted cross sections to achieve reasonable agreement with the data but the shape was poorly reproduced. In a subsequent publication, however, Shepard and Rost[23] were able to account reasonably well for these same data with an exact-finite-range single neutron transfer distorted wave calculation.

ACKNOWLEDGMENT

The authors wish to express their appreciation to H. S. Wilson and G. Hassold for their help in conducting the experiment. This work was supported in part by the US Department of Energy, the Natural Sciences and Engineering Research Council of Canada, and the US National Aeronautics and Space Administration.

* Present address: E. G. and G. Energy Measurements, Inc.
Los Alamos, NM 87545

** Present address: Lab. Nat. Saturne, CEN Saclay
91191 Gif-sur-Yvette, Cedex, France

References

1 J. R. Shepard, R. L. Boudrie, N. S. P. King, G. Igo, A. Rahbar, B. Aas, C. A. Witten, M. Gazzally and G. S. Adams, to be published.

2 M. Bernas, D. Bachelier, J. K. Lee, R. Radvanyi, M. Roy-Stéphan, I. Brissaud and C. Detraz, Nucl. Phys. A156, 289 (1970)

3 T. Bauer, A. Boudard, H. Catz, A. Chaumeaux, P. Couvert, M. Gardon, J. Guyot, D. Legrand, J. C. Lugol, M. Matoba, B. Mayer, J. P. Tabet and Y. Terrien, Phys. Let. 67B, 265 (1977)

4 A. W. Stetz, J. M. Cameron, D. A. Hutcheon, R. H. McCamis, C. A. Miller, G. A. Moss, G. Roy, J. G. Rogers, C. A. Goulding, and W. T. H. van Oers, Nucl. Phys. A290, 285 (19755).

5. R. H. McCamis, J. M. Cameron, L. G. Greeniaus, D. A. Hutcheon, C. A. Miller, G. A. Moss, G. Roy, M. S. de Jong, B. T. Murdoch, W. T. H. van Oers, J. G. Rogers, and A. W. Stetz, Nucl. Phys. A302, 388 (1978)

6. L. G. Greeniaus, D. A. Hutcheon, C. A. Miller, G. A. Moss, G. Roy, R. Dubois, C. Amsler, B. K. S. Koene, and B. T. Murdoch, Nucl. Phys. A322, 308 (1979).

7. C. A. Goulding, B. T. Murdoch, M. S. de Jong, W. T. H. van Oers, and R. H. McCamis, Nucl. Instrum. Meth. 148, 11 (1978).

8. R. H. McCamis, Ph.D. thesis, University of Alberta, 1977 (unpublished)

9. G. A. Moss, C. A. Davis, J. M. Greben, L. G. Greeniaus, G. Roy, J. Uegaki, R. Abegg, D. A. Hutcheon, C. A. Miller and W. T. H. van Oers, Nucl. Phys. A392, 361 (1983)

10. J. Kmline, J. Phys. G. Nucl. Phys. 8, 1371 (1982)

11. G. A. Moss, L. G. Greeniaus, J. M. Cameron, D. A. Hutcheon, R. L. Liljestrand, C. A. Miller, G. Roy, B. K. S. Koene, W. T. H. van Oers, A. W. Stetz, A. Willis and N. Willis, Phys. Rev. C. 21, 1932 (1980)

12. J. M. Cameron, L. G. Greeniaus, D. A. Hutcheon, R. H. McCamis, C. A. Miller, G. A. Moss, G. Roy, M. S. deJong, B. T. Murdoch, W. T. H. van Oers, J. G. Rogers and A. W. Stetz, Phys. Lett. 74B, 31 (1978)

13. L. G. Votta, P. G. Roos, N. S. Chant and R. Woody III, Phys. Rev. C 10, 520 (1974)

14. H. Coutant, K. Einsweiler, T. Joyce, H. Kagan, Y. I. Makdisi, M. L. Marshak, B. Mossberg, E. A. Peterson, K. Ruddick, T. Walsh, G. J. Igo, R. Talaga, A. Wriekat, and R. Klem, Phys. Rev. C 19, 104 (1979)

15. Program MAGALI, J. Raynal, private communication.

16. R. C. Johnson and P. J. R. Soper, Phys. Rev. C. 1, 976 (1970).

17. J. D. Harvey and R. C. Johnson, Phys. Rev. C 3, 636 (1971).

18. P. J. Brussard and D. W. M. Glaudemans, Shell Model Applications in Nuclear Spectroscopy (North-Holland, Amsterdam, 1977), p. 3.

19. V. A. Goldstein, Eh. L. Kuplennikov, R. I. Jubuti and R. Ya. Kezerashvili, Nucl. Phys. A355, 333 (1981).

20. J. R. Shepard, E. Rost and G. R. Smith, Phys. Lett. 89B, 13 (1979)

21. P. D. Kunz, University of Colorado, Unpublished.

22. A. Boudard, Y. Terrien, R. Beurtey, L. Bimbot, G. Bruge, A. Chaumeaux, P. Couvert, J. M. Fountaine, M. Gargon, Y. LeBornec, D. Legrand, L. Schecter, J. P. Tabet and M. Dillig, Phys. Rev. Lett. 46, 218 (1981).

23. J. R. Shepard and E. Rost, Phys. Rev. Lett. 46, 1544 (1981).

Table I

Cross sections and analyzing power data for the $^4He(\vec{p},d)^3He$ reaction at 200 and 400 MeV

θ_{cm}(deg)	$d\sigma/d\Omega(\mu b/sr.)_{c.m.}$	A_y
Ep=200 MeV		
23.4	495±6	-0.41±0.02
25.6	462±6	-0.25±0.02
29.3	389±5	0.01±0.02
32.9	312±4	0.08±0.02
36.5	246±3	0.15±0.02
40.1	167±3	0.16±0.03
43.6	97.7±0.8	0.25±0.01
47.1	64.7±0.7	0.17±0.01
50.6	42.3±0.4	0.16±0.01
54.1	30.9±0.3	0.11±0.02
57.6	23.9±0.2	0.15±0.01
61.0	20.4±0.2	0.22±0.02
64.3	17.4±0.2	0.29±0.02
67.7	14.4±0.2	0.40±0.02
71.0	12.5±0.2	0.44±0.02
74.2	11.0±0.2	0.48±0.03
77.5	9.4±0.2	0.51±0.03
80.6	7.9±0.2	0.56±0.04
83.8	6.4±0.3	0.59±0.05
89.9	5.1±0.2	0.61±0.07
Ep=400 MeV		
23.7	72±1	-0.32±0.02
26.0	56.3±0.9	-0.31±0.02
29.7	31.5±0.8	-0.34±0.02
33.4	17.2±0.3	-0.29±0.02
37.0	8.7±0.2	-0.03±0.03
40.6	6.1±0.1	0.25±0.03
44.2	4.5±0.1	0.44±0.04
47.8	3.59±0.07	0.51±0.03
51.3	3.05±0.08	0.39±0.04
54.8	2.47±0.07	0.29±0.04
58.2	2.04±0.07	0.35±0.05
61.7	1.67±0.06	0.33±0.05
65.1	1.55±0.04	0.25±0.03
68.4	1.26±0.06	0.28±0.07
71.7	1.11±0.06	0.35±0.08
75.0	0.99±0.03	0.47±0.05
78.2	0.85±0.04	0.52±0.06
81.4	0.82±0.03	0.57±0.06
84.5	0.78±0.05	0.66±0.09
96.6	0.42±0.04	0.62±0.14
107.7	0.17±0.03	0.51±0.30

Table II

Optical Model Parameters

T p (MeV)	Channel	V R (MeV)	r R (fm)	a R (fm)	W I (MeV)	r I (fm)	a I (fm)	V so (MeV)	r so (fm)	a so (fm)
156	p	-7.40	1.244	0.206	-13.45	1.494	0.336	-6.30	0.852	0.217
	d	-20.25	1.144	0.246	-18.09	1.72	0.40	-4.80	0.855	0.246
200	p	-3.64	1.244	0.206	-13.16	1.387	0.336	-5.75	0.857	0.228
	d	-16.650	1.164	0.246	-17.63	1.62	0.40	-4.54	0.853	0.249
400	p	+11.60	1.244	0.206	- 9.50	1.480	0.336	-4.56	0.940	0.303
	d	+ 1.650	1.244	0.246	-16.88	1.37	0.40	-3.60	0.860	0.307
770	p	+20.00	1.244	0.206	-10.20	1.278	0.336	-1.80	0.969	0.266
	d	+22.875	1.244	0.246	- 7.965	1.45	0.40	-2.37	0.980	0.336

Figure Captions

Figure 1 Angular distributions for the $^4He(p,d)^3He$ reaction taken with proton energies of 200 and 400 MeV. The solid lines are the results of exact-finite-range distorted wave calculations using a Gaussian shaped form factor for the bound state calculations and for the dashed line a form factor derived from electron scattering on ^4He was used. The open circles at 400 MeV are from Ref. 12.

Figure 2 Analyzing power data for the $^4He(\vec{p},d)^3He$ reaction at 200 and 400 MeV. The solid and dashed lines are the results of calculations described in Figure 1.

Figure 3 Angular distribution for the $^4He(p,d)^3He$ reaction at 156 MeV (Ref. 2). The solid and dashed lines are the results of calculations as described in Figure 1.

Figure 4 Angular distribution for the $^4He(p,d)^3He$ reaction at 770 MeV (Ref. 3). The solid and dashed lines are the results of calculations as described in Figure 1.

Figure 5 Diagrams illustrating various possible contributions to the $^4He(p,d)^3He$ cross section. The one and two nucleon transfer are shown in (a) and (b) respectively. The process of interaction through a delta is shown in (c) and (d) either directly with the transferred neutron or with a spectator.

Fig 1

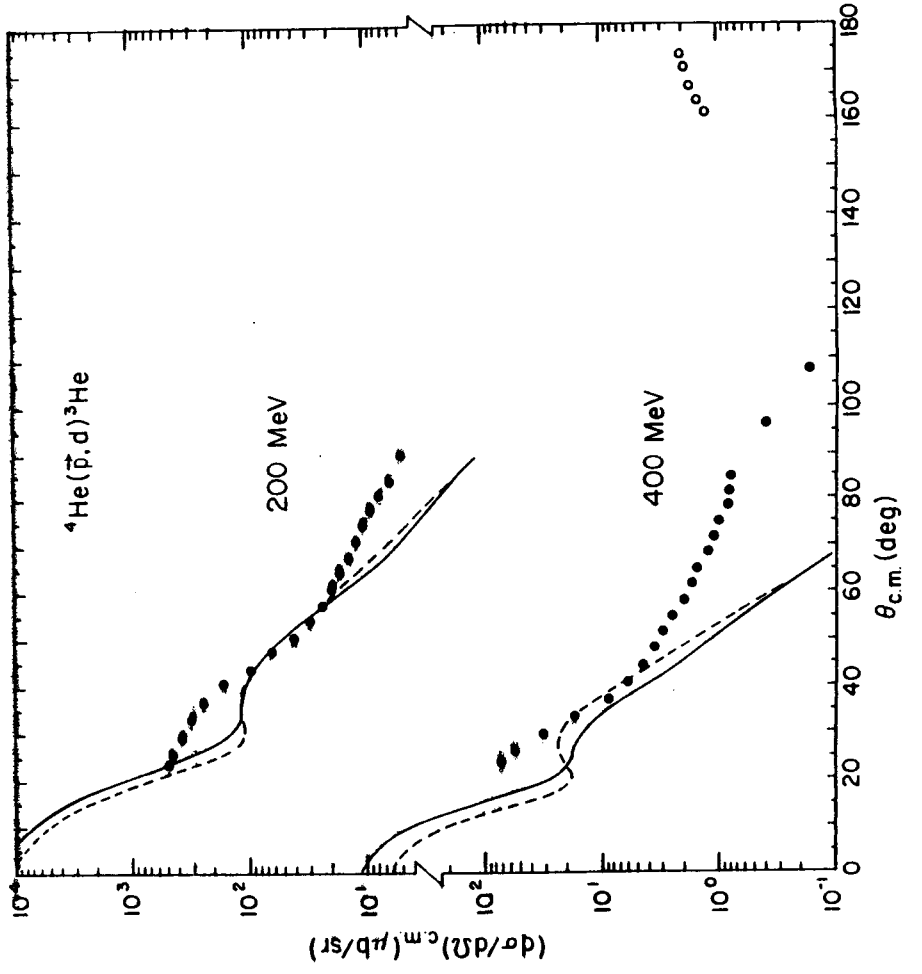

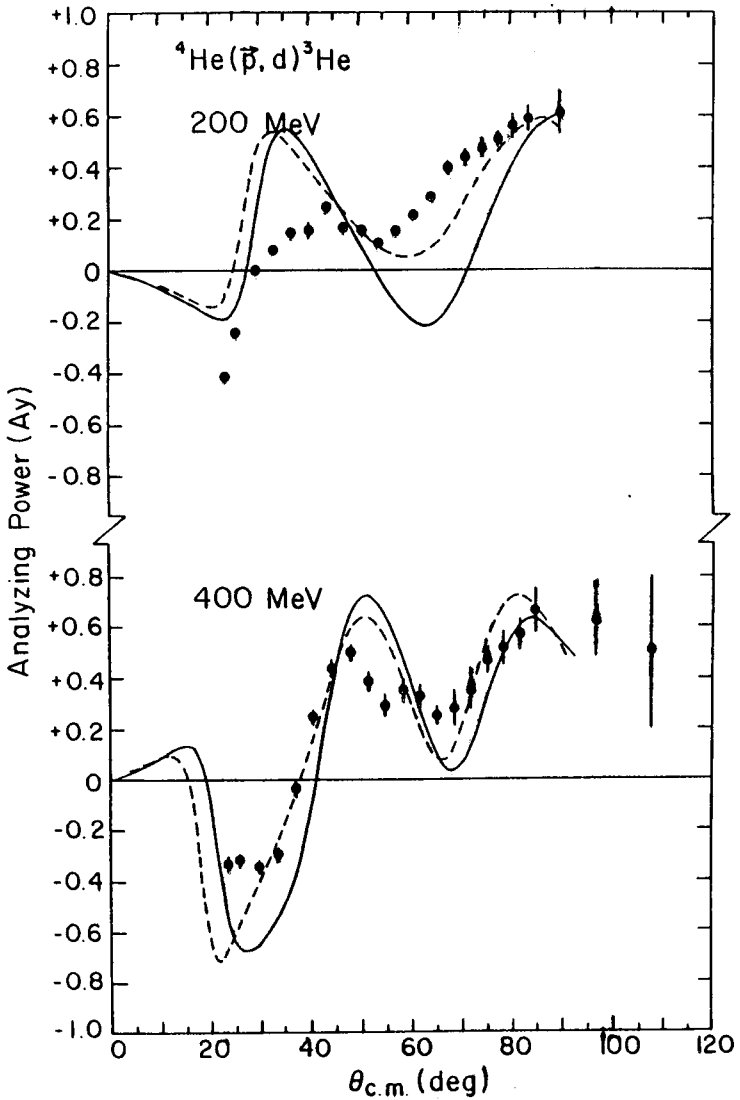
^{4}He($\vec{p}$, d)^{3}He
200 MeV
400 MeV
Analyzing Power (Ay)
$\theta_{c.m.}$ (deg)

Fig 2

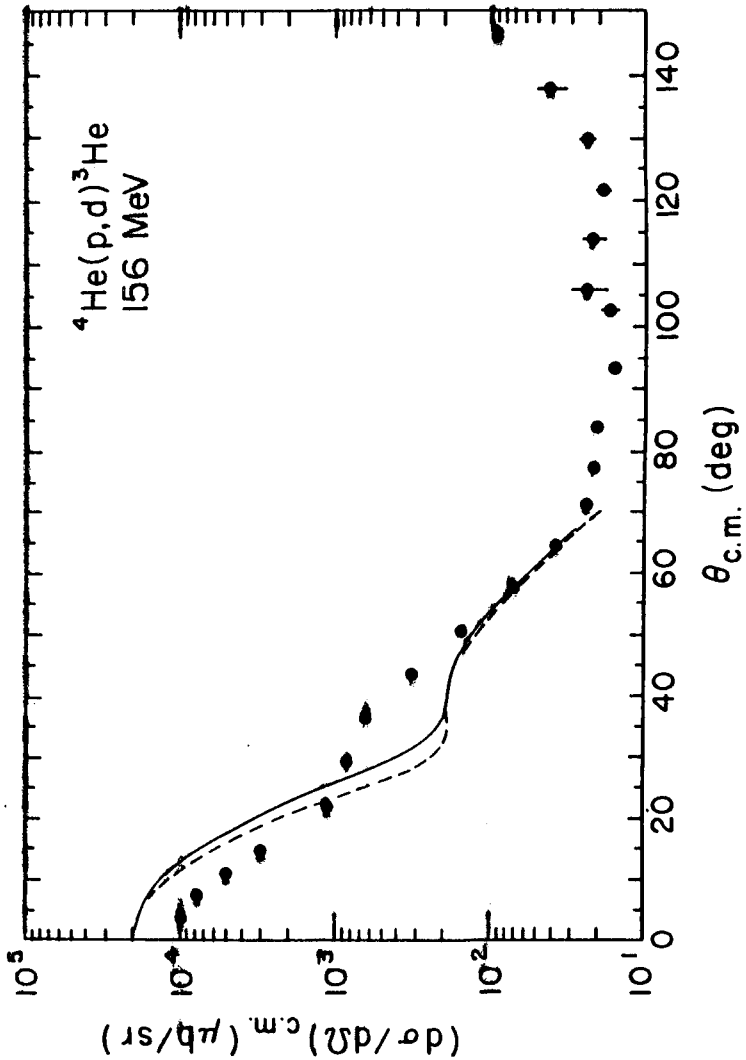
^{4}He(p,d)^{3}He
156 MeV
$(d\sigma/d\Omega)_{c.m.}$ (μb/sr)
$\theta_{c.m.}$ (deg)

Fig 3

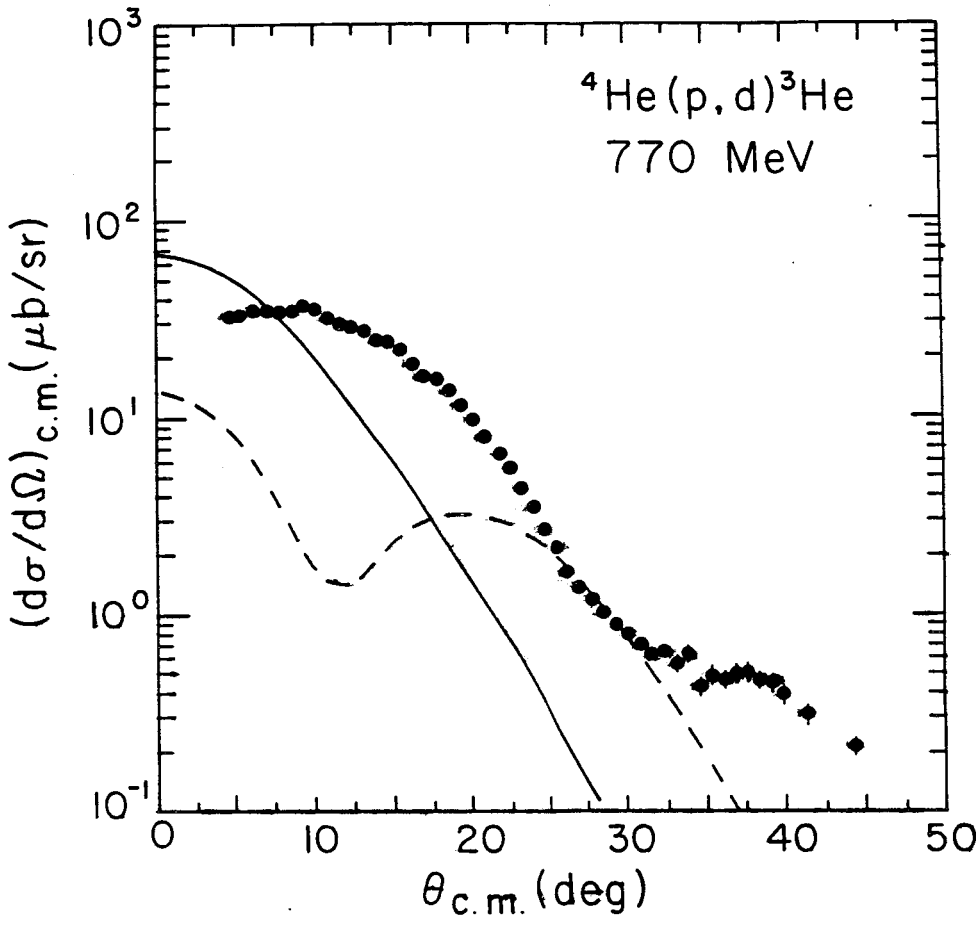
^{4}He(p,d)^{3}He
770 MeV
$(d\sigma/d\Omega)_{c.m.}$ (μb/sr)
$\theta_{c.m.}$ (deg)
10^3
10^2
10^1
10^0
10^{-1}
0
10
20
30
40
50

Fig 4

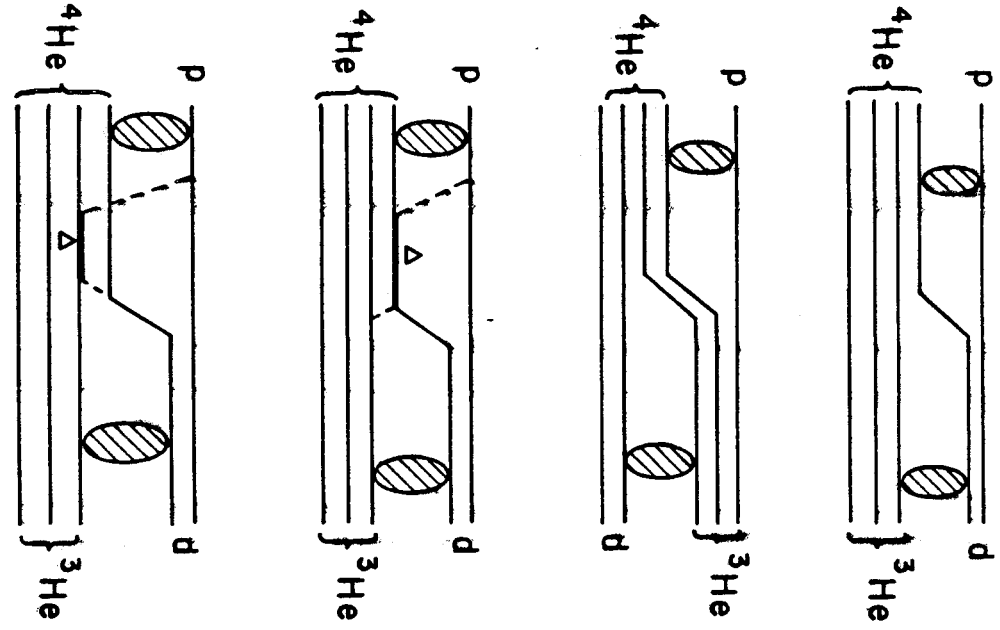
^{4}He
p
d
^{3}He
Δ
(a)
(b)
(c)
(d)

Fig 5